VOLUME 32 NOVEMBER 1954 NUMBER 11

Canadian Journal of Physics

Published by THE NATIONAL RESEARCH COUNCIL
OTTAWA CANADA

CANADIAN JOURNAL OF PHYSICS

(Formerly Section A, Canadian Journal of Research)

Under the authority of the Chairman of the Committee of the Privy Council on Scientific and Industrial Research, the National Research Council issues annually THE CANADIAN JOURNAL OF PHYSICS and six other journals devoted to the publication of the results of original scientific research. Matters of general policy concerning these journals are the responsibility of a joint Editorial Board consisting of: members representing the National Research Council of Canada; the Editors of the Journals; and members representing the Royal Society of Canada and four other scientific societies.

Manuscripts for publication should be submitted to Dr. Léo Marion, Editor-in-Chief, Canadian Journal of Physics, National Research Council, Ottawa 2, Canada.
(For instructions on preparation of copy, see **Notes to Contributors** (inside back cover).)

Proof, correspondence concerning proof, and *orders for reprints* should be sent to the Manager, Editorial Office (Research Journals), Division of Administration, National Research Council, Ottawa 2, Canada.

Subscriptions, renewals, and orders for single or back numbers should be sent to Division of Administration, National Research Council, Ottawa 2, Canada. Remittances should be made payable to the Receiver General of Canada, credit National Research Council.

The journals published, frequency of publication, and prices are:

Canadian Journal of Biochemistry and Physiology	Bimonthly	$3.00 a year
Canadian Journal of Botany	Bimonthly	$4.00 a year
Canadian Journal of Chemistry	Monthly	$5.00 a year
Canadian Journal of Microbiology*	Bimonthly	$3.00 a year
Canadian Journal of Physics	Monthly	$4.00 a year
Canadian Journal of Technology	Bimonthly	$3.00 a year
Canadian Journal of Zoology	Bimonthly	$3.00 a year

The price of single numbers of all journals is 75 cents.

*Volume 1 will combine three numbers published in 1954 with six published in 1955 and will be available at the regular annual subscription rate of $3.00.

Canadian Journal of Physics

Issued by THE NATIONAL RESEARCH COUNCIL OF CANADA

VOLUME 32 NOVEMBER 1954 NUMBER 11

THE POTASSIUM–ARGON METHOD OF GEOLOGICAL AGE DETERMINATION[1]

BY H. A. SHILLIBEER AND R. D. RUSSELL

ABSTRACT

The development of the potassium–argon method for dating minerals is discussed. The decay scheme for radioactive potassium-40 is examined. The results of 11 recent counting experiments have been averaged and give a mean value of 29.4 ± 2.7 beta emissions per second per gram of potassium. Averaging the 15 previous determinations of the rate of gamma decay gives a branching ratio of 0.090 ± 0.038 with the above beta decay rate. This is in close agreement with a branching ratio of 0.089 suggested by us in a previous paper on the basis of two potassium–argon determinations.

Methods of measuring the radiogenic argon content of potassium minerals are discussed and the method in use at this laboratory is described in detail. Yield runs and grain size experiments have been carried out and are reported. Potassium–argon ages have been calculated for four perthites and two lepidolites. These ages are in excellent agreement with the best available ages obtained by other methods.

INTRODUCTION

Two years after the discovery by Thomson that a sodium–potassium alloy spontaneously emitted negative particles, Campbell and Wood conclusively proved the radioactivity of potassium (46). Particularly since the proof of its decay to argon by Thompson and Rowlands (47), geophysicists have been keenly aware of the great possibilities of a potassium–argon method of age determination. Such a method would permit dating of a wide variety of minerals and rocks which contain appreciable amounts of potassium, and would permit more detailed studies of geological history than have ever been possible before.

Both calcium-40 and argon-40 are produced by the decay of potassium-40. But calcium is a very common constituent of rocks and minerals, and calcium-40 forms 97% of common calcium. As a result it is very difficult to distinguish a small amount of radiogenic calcium from the larger amount of common calcium usually present, and a potassium–calcium age-scale would be of limited use. However no such objection applies to the potassium–argon method because the amount of common argon contained in minerals is very small. Moreover argon is a gas and its measurement in small quantities (10^{-4} to 10^{-5} gm.) presents fewer difficulties than would be encountered in analyzing for small quantities of calcium.

[1]*Manuscript received July 7, 1954.*
Contribution from the Department of Physics, University of Toronto, Toronto, Ontario.

Unfortunately the establishment of an argon method of dating has been complicated by a number of practical problems. The quantitative extraction and purification of the radiogenic argon is extremely difficult. The first attempt at such measurement was made by Harteck and Suess (19) who failed to find argon in dated potassium minerals. Farrar and Cady (9) reported the results of a number of determinations which showed no relationship between the amounts of potassium and argon and the age of minerals. The existence of such a relationship was first demonstrated by Aldrich and Nier (2), who used their results to find approximate values for the decay constants of potassium-40. Mousuf (31) first showed the very high radiogenic purity of argon found in old potassium feldspars.

Another difficulty has been the fact that the decay constants of potassium have not been precisely determined by physical measurements. Until this is done it will be impossible to prove conclusively that small quantities of argon are not lost by diffusion from the minerals and a potassium–argon time-scale cannot be put on an independent basis.

Despite these and other difficulties the future of the potassium–argon method has never looked brighter. The great differences that once existed between geophysical and physical values for the potassium-40 decay constants are rapidly disappearing, and provisional potassium–argon ages have been in reasonable accord with those obtained by other methods. Within the past four years radiogenic argon measurements have been reported by Smits and Gentner (42), Gerling and Pavlova (14), Fritze and Strassmann (12), Gentner, Prag, and Smits (13), Russell, Shillibeer, Farquhar, and Mousuf (37), Wasserburg and Hayden (48), and Shillibeer, Russell, Farquhar, and Jones (40).

The purpose of this paper is to review the present status of potassium–argon dating and to report the results of new measurements which strongly support this new method of determining geological ages.

THE RADIOACTIVITY OF POTASSIUM

Geological ages based on any radioactive decay demand an accurate knowledge of the decay rates of the element concerned. Potassium-40 decays by both beta emission and orbital electron capture to calcium and argon respectively. A knowledge of two decay constants is necessary to predict the rate of accumulation of either calcium or argon. It is convenient to use the branching ratio R, which is the ratio of orbital electron captures to beta emissions, and the decay constant for beta emission λ_β. Using these decay constants, the accumulation of radiogenic argon in a potassium mineral is given by

$$A^{40}/K^{40} = \{R/(1+R)\}\{\exp(1+R)\lambda_\beta t - 1\}.$$

λ_β is directly proportional to the number of beta particles emitted from one gram of potassium in unit time. This has been measured many times by a number of workers. The more recent determinations, which are listed in Table I, are in reasonable agreement. The mean of these results gives a beta decay constant of 0.503×10^{-9} years^{-1} with a standard deviation of approximately nine per cent.

TABLE I

RATE OF BETA EMISSION BY POTASSIUM

Year	Authority	β's/sec. gm. K
1948	Borst and Floyd (4)	23 $\pm$ 2*
	Gråf (16)	26.8 $\pm$ 1.2
	Hirzel and Wäffler (21)	34 $\pm$ 4
1949	Floyd and Borst (11)	25 $\pm$ 2
	Stout (44)	30.6 $\pm$ 2.0
1950	Faust (10)	31.2 $\pm$ 3.0
	Houtermans, Haxel, and Heintz (24)	27.1
	Sawyer and Wiedenbeck (39) (ordinary potassium)	28.3 $\pm$ 1
	Sawyer and Wiedenbeck (39) (enriched to 0.4% K^{40})	30.9 $\pm$ 1.7
	Smaller, May, and Freedman (41)	23*
	Spiers (43)	30.5
1951	Delaney (8)	32.0 $\pm$ 3.0
	Good (15)	27.4
		Mean $\pm$ standard deviation = 29.4 $\pm$ 2.7

*These results were omitted in calculating the mean.

The branching ratio can be determined by dividing the rate of orbital capture by this rate of beta emission. In theory the rate of capture can be most directly determined by counting the number of X-rays and Auger electrons, one of which is emitted by the argon atom formed during each capture process. In practice both X-rays and Auger electrons are extremely difficult to count, and no precise measurements have been made.

However there seems to be good reason to believe that the rate of orbital electron capture is equal to the rate of gamma-ray emission. This is supported by precision mass measurements of Johnson (26), which show that only one gamma ray can be associated with an electron capture and that none can be associated with a beta emission. It has also been supported on theoretical grounds by Morrison (30). These recent results suggest that the branching ratio can be estimated directly from the results of beta particle and gamma ray counting experiments, as suggested by Bramley (5) nearly twenty years ago.

Although these gamma rays are much more easily counted than argon X-rays, the results from gamma ray counting experiments have not been in very good agreement. The values for the branching ratios estimated in this way are summarized in Table II. All have been calculated with the average rate of beta decay obtained in Table I. Where the same author or authors have reported more than one result, the more recent value has been used; otherwise the list is complete to the best of our knowledge. The average value for the branching ratio calculated from these measurements is 0.090 with a standard deviation of $\pm$0.038. It is obvious that results could be selected to give almost any branching ratio within this range.

Two branching ratio measurements deserve special comment. The first is the Auger electron counting experiment of Sawyer and Wiedenbeck (39). This experiment more than any other indicated the equality between the branching ratio and the ratio of gamma rays to beta particles. However the experimental error assigned by the original authors ($\pm$30%) is large enough

TABLE II

RATE OF GAMMA RAY EMISSION BY POTASSIUM

Year	Authority	Quantity measured			Branching ratio
		γ radiation (curies/gm.K)	γ's/sec. gm. K	$\lambda_\gamma/\lambda_\beta$	
1930	Köhlhorster (28)	5×10^{-11}			0.061
	Mühloff (32)	3.3×10^{-11}			0.040
1931	Běhounek (3)	1.3×10^{-10}			0.16
1934	Gray and Tarrant (18)	1.6×10^{-11}			0.02
1948	Ahrens and Evans (1)		3.3		0.11 (2)
	Gràf (17)		3.4 ± 0.8		0.11(5) $\pm$ .025
	Hess and Roll (20)	8.9×10^{-11}			0.10 (9)
	Hirzel and Wäffler (21)			$0.087 \pm .012$	$0.087 \pm .012$
1949	Floyd and Borst (11)			$0.05 \pm .01$	$0.05 \pm .01$
	Sawyer and Wiedenbeck (38)		2.9 ± 0.3*		$0.098 \pm .010$
1950	Faust (10)		3.6 ± 0.4		$0.122 \pm .014$
	Houtermans, Haxel, and Heintz (24)		3.1 ± 0.3		$0.105 \pm .010$
	Smaller, May, and Freedman (41)			$0.05 \pm .01$	$0.05 \pm .01$
	Spiers (43)		3.0		0.10 (2)
1953	Burch (6)		3.4–3.6		$0.119 \pm .006$
				Mean $\pm$ standard deviation =	0.090 ± 0.038

**This value has been recalculated from the original data using a more recent value for the gamma activity of potassium-42 (27).*

to cause considerable uncertainty in potassium–argon ages. The second determination is the radiogenic calcium and argon measurements made on a sample of Stassfurt sylvite by Inghram, Brown, Patterson, and Hess (25). They carried out the experiment by measuring both the radiogenic calcium and argon with a mass spectrometer by isotopic dilution and obtained a value of $0.126 \pm .002$ for the branching ratio. Although this experiment seems very good there appear to be two inconsistencies. First, the figures obtained by Inghram's group indicate an age of 90 million years for the sylvite, if it is approximately 100% potassium chloride. However the Stassfurt deposits are classed geologically as mid- to late-Permian (29). The age of the Permian period has been well established at 200 to 220 million years (22), more than twice the age obtained by Inghram. Since in this experiment the branching ratio is determined by the argon measurement, the discrepancy in the age cannot be removed by assuming that the radiogenic argon was measured incorrectly, but can be explained by assuming that the mineral was not Permian in age, or that the radiogenic calcium figure was too low. If the radiogenic calcium figure was too low the branching ratio obtained would be too large.

The second inconsistency is shown by studies of Gentner, Prag, and Smits (13) which indicate that argon diffuses from sylvites with a diffusion constant of 10^{-19} sq. cm. per sec. This value was calculated using a branching ratio of 0.13. Unfortunately there is no record of the grain size of the sylvite used by Inghram, but if a grain size of 2 mm. is assumed, the mean size of Gentner's

samples, a loss of 42% of the argon would be expected. If the grain size is taken as 4 mm., the maximum size reported by Gentner, the loss would be 28%. If so much argon had been lost from Inghram's sample the branching ratio calculated from his figures would be impossibly large.

If sufficient suitable samples can be found, this method may eventually prove to be best, but the result obtained by Inghram, Brown, Patterson, and Hess will be in some doubt until these inconsistencies are removed.

METHODS OF POTASSIUM–ARGON DATING

For calculating potassium–argon ages it is convenient to use the decay equation in the form

$$t = \frac{1}{(1+R)\lambda_\beta} \log_e\left(1 + \frac{(1+R)A^{40}}{RK^{40}}\right).$$

A^{40} represents the mass of radiogenic argon-40 present per gram of mineral sample. In general the gases present in the mineral, including argon, are extracted from it by fusing in a high vacuum system. The major part of the impurities are then removed. If the purification is carried out so that only argon remains, then the volume of argon may be measured by means of a McLeod gauge. Alternatively, a known volume of argon-38 (or argon-36) may be added to the unpurified gases from the sample and the volume of the radiogenic argon calculated from mass spectrometer measurements. In any case, a mass spectrometer analysis is necessary in order to correct for the presence of non-radiogenic argon. The present authors use the McLeod gauge method, the details of which will be described below.

K^{40} represents the mass of potassium-40 per gram of sample. Nier (34) found that this isotope forms 0.0119% of common potassium, which value has been substantiated by Reuterswärd (35) who obtained 0.0118%. Nier's result has been used for all our calculations. The total potassium content is determined by a chemical analysis.

λ_β, the partial decay constant for beta emission, has been discussed earlier in this paper. The value of $0.503 \pm .046 \times 10^{-9}$ years^{-1} obtained from the measurements in Table I has been used for all calculations.

The value for R, the branching ratio, obtained by averaging the results of all gamma ray counting experiments (Table II) was $0.090 \pm .038$. A value of 0.088 was obtained by combining potassium–argon measurements reported by Wasserburg and Hayden (48) for Besner Mine, Ontario, with a lead-ratio age determination carried out at Toronto on a uraninite found with the feldspar. The latter paper also reported a calculation for a dated feldspar from Lee Lake, Saskatchewan, which gave a branching ratio of 0.090. In view of these results we have chosen a tentative branching ratio of 0.089 for our calculations.

EXPERIMENTAL PROCEDURE

Potassium Analyses

Some of the potassium analyses used in this paper were carried out on a flame photometer by Mr. W. R. Inman of the Department of Mineral Dressing

and Process Metallurgy, Ottawa. Mr. Inman has checked the accuracy of his method by using standard feldspars of known potassium content obtained from the U.S. National Bureau of Standards. Other analyses have been made on a flame photometer recently constructed at Toronto by J. F. Sturm. Several comparisons have been made by Sturm on the same samples analyzed by Inman. Some of these are given in Table III. At present we consider that

TABLE III

INTERCOMPARISON OF POTASSIUM ANALYSES

Sample No.	$\%K_2O$	
	Ottawa	Toronto
1069	13.07	13.05
1063	10.96	11.1
1025	4.38	4.07
1059	12.25	12.01

our potassium analyses are in error by not more than 7%. Since any errors in these analyses result in errors in the ages, we are endeavoring to decrease this uncertainty.

The samples from Varala, Finland, were analyzed chemically by Mr. H. B. Wiik of the Geological Survey of Finland.

The Extraction and Purification of the Radiogenic Argon

A sample of the mineral was finely crushed and placed in a container with at least double its weight of sodium hydroxide flux. The container was then bolted to a vacuum line and evacuated to a pressure of approximately 10^{-3} mm. of mercury. The sample container was then disconnected from the pumping system by means of a stopcock, and was connected through a cold trap to a U-trap containing degassed activated charcoal. Both the cold trap and the U-trap were kept at the temperature of liquid air. At liquid air temperature and low pressure activated charcoal adsorbs more than 99.9% of the small volume of argon present. No argon condenses at this temperature and pressure without the presence of activated charcoal. This property of activated charcoal enables us to use an extraction line in which the argon can be transferred to any desired section by simply surrounding a charcoal trap with a Dewar flask containing liquid air. The main purpose of the cold trap was to remove the water released by the reaction of sodium hydroxide with the mineral and to prevent the water from reaching the charcoal trap.

The sample was heated to approximately 850°C. at which temperature the mixture was completely liquid and could be stirred with a metal rod. It was maintained at this temperature for 12 hr. Water and some other impurities were removed by the cold trap while all the argon was adsorbed by the activated charcoal in the U-trap section. The gases in the U-trap section were then purified with a calcium furnace. The calcium was heated by means of an induction heater to about 800°C., at which temperature calcium vapor

reacted rapidly with all gases, except noble gases, to form solid products which were deposited on the walls of the calcium furnace.

After purification the volume of the remaining gas was measured in a McLeod gauge. To ensure that purification was complete the sample was repurified and then remeasured. To ensure that none of the other noble gases were present a photograph of the line spectrum of one of the samples was taken. This showed only the line spectrum of argon and mercury, the mercury lines being due to the free mercury used in the McLeod gauge.

The sample was then adsorbed on charcoal in a break seal tube and the tube cut off so that the radiogenic purity of the argon could be measured mass spectrometrically. A measure of the relative abundances of argon-40 and argon-36 atoms contained in the sample enables one to make a correction for any contamination of the sample by atmospheric argon. This correction was in most cases less than 10% and often less than 5%. Most of this contamination is probably due to insufficient pumping on the sample at the beginning of a run but part of it may be argon trapped in the mineral at the time of formation. Several samples were also checked on the mass spectrometer for hydrogen, helium, and krypton and none of these gases was ever found.

Knowing the potassium and argon content of a given weight of mineral and the decay constants of K^{40} the age of the mineral can be calculated.

The Problem of Argon Loss

The argon measurement will be correct if the following three conditions are satisfied.

(1) None of the argon has escaped before the sample was heated in the container.

(2) All the argon was extracted from the mineral.

(3) None of the argon was lost during the purification process.

The last of these conditions is easily checked by carrying out yield runs. A sample was placed in the container, run in the normal way, and the volume of argon measured. This measured volume was then taken back to the U-trap and frozen down again. A second identical sample was placed in the container and also run in the normal way. After purification the measured volume was twice the volume of the single sample. This showed conclusively that none of the sample was lost during the purification process.

It is more difficult to prove that all the argon is being extracted from the mineral, but the experimental results indicate that this is the case. The consistency of the results obtained with the sodium hydroxide flux is one such indication. This is supported by results obtained from the same samples run with solid sodium as a flux. The A^{40}/K^{40} ratios obtained for the latter samples are also given, in Table IV. In this case the amount of argon extracted increases as the sample becomes more finely crushed, and the volume extracted from the finest sample closely approaches the mean result obtained with the sodium hydroxide flux. This indicates that even with solid sodium as a flux complete extraction is being approached under these conditions. Potassium feldspars and lepidolites, different minerals with completely different lattice structures,

TABLE IV

EFFECT OF VARYING SAMPLE MESH SIZE

Mesh size	Measured diameter of grains	Solid sodium flux		Sodium hydroxide flux	
		No. of runs	A^{40}/K^{40}	No. of runs	A^{40}/K^{40}
20–60				2	0.140
60–100	0.021	2	0.070	1	0.137
100–200	0.017	2	0.093	2	0.137
200–250	0.010	2	0.108		
		2	0.119		
250	0.002	2	0.134	1	0.137

Mean ± standard deviation = 0.138 ± .002

both give ages agreeing with established uranium ages. This suggests that the lattice structures have in both cases been completely broken down by the sodium hydroxide flux.

The good agreement between branching ratio values calculated from one of our measurements and a measurement by Wasserburg and Hayden (48) constitutes a check on the whole extraction and purification method (40). The two laboratories use entirely different purification and measuring methods, and hence the agreement can be most easily explained by assuming that both laboratories are extracting and measuring all the argon contained in the samples. Wasserburg and Hayden use a sodium hydroxide flux and an argon-38 spike in an isotopic dilution method first used by Suess, Hayden, and Inghram (45). We used a McLeod gauge measurement after complete purification of the argon in the manner already described.

The last important indication that all the argon is extracted is the agreement obtained between the branching ratio measured by counting experiments (Table II) and the results we obtain by using minerals of a known age (40). The mean result obtained from counting experiments is 0.09 ± .038 and the result obtained from two minerals of known age was 0.089. This agreement is much better than could be expected in view of the large scatter in the results from the counting experiments; it may be purely fortuitous.

It has been suggested that part of the argon may be driven into the walls of the calcium furnace by a glow discharge caused by the induction heater. We have operated three different calcium furnaces with two different induction heaters and have never observed any glow discharge. This possibility of argon loss was checked by the yield runs just described and also by sparking the argon by means of a Tesla coil. In neither case was argon loss observed.

Loss of argon from the sample before its actual extraction may have occurred during the geologically long period since the formation of the mineral. During that time argon could possibly have been lost by diffusion into the surrounding rock. It is difficult to test this experimentally but the consistency of our experimental results for lepidolites and feldspars of greatly differing ages indicates that any possible diffusion loss must be small. Loss of argon may also have occurred during the much shorter period from the crushing of the sample and the placing of it in the sample container to the evacuation of the system.

To show that no argon was lost owing to the initial pumping different samples of the same mineral were pumped for 5 min., 3 hr., and 24 hr. The results agreed within the experimental errors.

The possibility of argon loss due to the crushing was tested by grinding samples to different grain sizes. The results of these tests are shown in Table IV. It can be seen that the amount of argon extracted was constant within the experimental error when the sodium hydroxide flux was used. This indicates that no argon was lost from the sample because of the crushing.

RESULTS

Six ages obtained by the potassium–argon method as described above are shown in Table V. Every sample was run at least twice and the standard deviation of the individual argon measurements is given. Where other ages existed for the same localities, these are shown in the table as "comparison ages".

The Lee Lake perthite was obtained from a pegmatite a few miles north of the northeast shore of Lac La Ronge. A uraninite was obtained from the same pegmatite. This uraninite has been dated at Toronto by the lead-ratio method and an age of 1740 ± 50 million years obtained. The potassium–argon age for this sample is 1750 million years. This sample is one of two used by us recently to determine the branching ratio of potassium-40 (40). It can be seen that the decay constants which we are at present using give a potassium–argon age in excellent agreement with the lead-ratio value.

The Silver Leaf Mine is a small pegmatite mine on the Winnipeg River a few miles upstream from the power dam at Pointe de Bois. It has at various times been called the Bear Claim and the Bob Claim and is shown under these names on provincial claim maps. It is situated approximately one-half mile from Huron Claim, which has been dated many times by the various lead–thorium–uranium methods. Of these determinations only those based on the radiogenic Pb^{207}/Pb^{206} ratio have given a consistent value. A uraninite and a monazite from the Huron Claim were analyzed isotopically by Nier (33). From his figures we calculated ages of 2475 and 2590 million years respectively for these minerals. A second uraninite obtained independently by the writers has been analyzed at this laboratory and a lead-ratio age of 2590 million years obtained. The potassium–argon age of 2550 million years for the Silver Leaf Mine lepidolite appears to be in excellent agreement with the lead ages for Huron Claim.

Holmes (23) has recently published the following age determinations made on Rhodesian monazites:

	$\frac{207}{206}$	$\frac{206}{U}$	$\frac{207}{U}$	$\frac{208}{Th}$
Ebonite Claims, Bikita, Southern Rhodesia	2680	2675	2680	2645
Jack Tin Claims, north of Salisbury, Southern Rhodesia	2650	2260	2470	1940
Irumi Hills, Northern Rhodesia	2620	2040	2330	1340

TABLE V

POTASSIUM–ARGON AGES

Toronto number	Location	Mineral	Longitude Latitude	% by wt. rad. A^{40} (*a*)	No. of runs	% by wt. K_2O	A^{40}/K^{40}	Age (*b*)	Comparison age	
1061–A	Lee Lake, Lac La Ronge, Saskatchewan	Perthite	104°20′W. 55°15′N.	$15.8 \pm 0.2 \times 10^{-5}$	3	12.02	0.130	1730 ± 120	1740 ± 50	(*c*)
1069–A	Moose Claims, Yellowknife, N.W.T.	Perthite	112°12′W. 62°11′N.	$24.6 \pm 1.9 \times 10^{-5}$	4	13.07	0.186	2160 ± 140	2160 ± 150	(*d*)
1080–A	Silver Leaf Mine, Winnipeg River, Manitoba	Lepidolite	95°22′W. 50°21′N.	$26.5 \pm 0.1 \times 10^{-5}$	2	10.1	0.259	2550 ± 150	2550 ± 70	(*e*)
1084–A	Popes Claim, Salisbury, S. Rhodesia	Lepidolite	31°05′E. 17°40′S.	$23.3 \pm 1.0 \times 10^{-5}$	2	8.6	0.268	2660 ± 150	2610 ± 75	(*f*)
1107–A	Dill Township, Ontario	Perthite	80°50′W. 46°24′N.	$6.57 \pm 0.32 \times 10^{-5}$	8	12.56	0.052	900 ± 70	Grenville	(*g*)
1149–A 1150–A 1151–A 1152–A 1153–A	Varala, Kangasala, Finland	Perthite	24° 5′E. 61°27′N.		6		0.138	1820 ± 120	None	

NOTES

(*a*) *Uncertainty shown is standard deviation of individual measurements.*

(*b*) *Limits of uncertainty based on estimated mean probable error of ±10% in A^{40}/K^{40} ratio. They do not include uncertainties in decay constants which could raise or lower all calculated ages proportionately.*

(*c*) *Lead-ratio age determination on same pegmatite.*

(*d*) *Mean and standard deviation of eight unpublished galena ages for Yellowknife area.*

(*e*) *Mean and standard deviation of three lead-ratio ages for Huron Claim, Manitoba.*

(*f*) *Mean and standard deviation of four lead-ratio ages for Southern Rhodesia.*

(*g*) *See, for example, Collins, Farquhar, and Russell (7).*

As is generally the case for old samples, the Pb^{207}/Pb^{206} ratio gives the only consistent ages. The excellent agreement for ages of the Bikita sample suggest that this is a very precise determination. Although this locality is some 50 miles from Popes Claim, there is some reason for believing that the areas may be parts of a single orogenic belt (23). A single sample of microlite has been obtained from Popes Claim and a lead-ratio age determined for it at Toronto. The age obtained was 2510 ± 100 million years. The potassium–argon age for Popes Claim lepidolite was found to be 2650 million years. Again the agreement between the two methods of geological age determination seems to be very satisfactory.

To the writers' knowledge no uranium minerals are available from the Yellowknife area for age determinations. However a number of ages have been calculated from galenas found in this area by the method suggested by Russell, Farquhar, Cumming, and Wilson (36). The mean of eight of these age determinations is 2160 million years with a standard deviation of 150 million years. The age obtained by the potassium–argon method for the Moose Dike pegmatite is 2160 million years. The potassium–argon method appears to best advantage in such areas as this where uranium minerals are exceedingly rare.

Dill Township, Ontario, is in the Grenville Geological province. The age of the Grenville orogeny has been assumed to be between 800 and 1100 million years (7). The potassium–argon age of 900 million years therefore does not seem unreasonable.

CONCLUSIONS

The measurements in this paper have been presented to illustrate the enormous potentialities of the potassium–argon method of dating and to show that present techniques are adequate to provide dates with fair precision. It is not suggested that the method is yet established, nor that the ages obtained will always be correct. However, wherever comparisons can be made between potassium–argon ages and ages calculated by other methods, the agreement is striking.

The rate of beta decay for potassium-40 was determined by averaging the results of a number of counting experiments. The branching ratio used was previously chosen to give agreement between lead-ratio ages and potassium–argon ages for two samples analyzed independently at two laboratories. The fact that these same decay constants give good agreement for samples of other ages indicates that they may be well chosen. More precise counting results would provide a much more stringent test of the potassium–argon method.

The assessment of potassium–argon ages is complicated by the fact that various age determination methods often give discordant results for the same location. The writers know of no method that gives invariably good results, nor for that matter, of any method that gives invariably bad results. However a good estimate of the correct age can often be made from a number of determinations carried out in the same area. Such comparisons have shown that for ages over one thousand million years the lead-ratio method gives much

more consistent results than the other uranium or thorium methods (7). For this reason we prefer to use lead-ratio ages to date our old samples wherever such ages exist. The "galena method" (36) is less well established, but it has given apparently good ages for old lead minerals, and we have used these ages for the Yellowknife area where no other ages have been determined.

Potassium–argon studies are being continued at this laboratory, and at several others. It seems certain that many new determinations will be reported very soon and that further tests of the potassium–argon method will be possible. It is also likely that the method will be soon applied to potassium-bearing rocks as well as to potassium–bearing minerals. Such tests may have an important bearing on the future course of geochronology.

ACKNOWLEDGMENTS

The writers wish to acknowledge the help and advice of Professor J. T. Wilson and Dr. R. M. Farquhar and E. A. W. Jones. Technical assistance from D. E. Beuk, W. J. Kenyon, and Mrs. R. S. Waddington played an important part in these investigations.

We are indebted to Dr. R. W. Boyle, G. L. Cumming, Dr. A. A. Kahma, Dr. J. B. Mawdsley, Dr. A. M. McGregor, and Dr. R. B. Rowe who supplied the samples used. W. R. Inman, D. A. Moddle, J. F. Sturm, and H. B. Wiik carried out the potassium analyses for us.

Financial assistance was received from the National Research Council of Canada, the Research Council of Ontario, the Geological Survey of Canada, and Imperial Oil Limited.

REFERENCES

1. AHRENS, L. H. and EVANS, R. D. Phys. Rev. 74: 279. 1948.
2. ALDRICH, L. T. and NIER, A. O. Phys. Rev. 74: 876. 1948.
3. BĚHOUNEK, F. Z. Physik, 69: 654. 1931.
4. BORST, L. B. and FLOYD, J. J. Phys. Rev. 74: 989. 1948.
5. BRAMLEY, A. Science, 86: 424. 1937.
6. BURCH, P. R. J. Nature, 172: 361. 1953.
7. COLLINS, C. B., FARQUHAR, R. M., and RUSSELL, R. D. Bull. Geol. Soc. Amer. 65: 1. 1954.
8. DELANEY, C. F. G. Phys. Rev. 81: 158. 1951; Sci. Proc. Roy. Dublin Soc. 25: 251. 1951.
9. FARRAR, R. L. and CADY, G. H. J. Am. Chem. Soc. 71: 742. 1949.
10. FAUST, W. R. Phys. Rev. 78: 624. 1950.
11. FLOYD, J. J. and BORST, L. B. Phys. Rev. 75: 1106. 1949.
12. FRITZE, J. and STRASSMANN, F. Naturwiss. 39: 522. 1952.
13. GENTNER, W., PRAG, R., and SMITS, F. Z. Naturforsch. 8a: 216. 1953.
14. GERLING, E. K. and PAVLOVA, T. G. Doklady Akad. Nauk S.S.S.R. 77: 85. 1951.
15. GOOD, M. L. Phys. Rev. 83: 1054. 1951.
16. GRÀF, T. Phys. Rev. 74: 831. 1948.
17. GRÀF, T. Phys. Rev. 74: 1199. 1948.
18. GRAY, L. H. and TARRANT, G. T. P. Proc. Roy. Soc. (London), A, 143: 681. 1934.
19. HARTECK, P. and SUESS, H. E. Naturwiss. 34: 214. 1947.
20. HESS, V. F. and ROLL, J. D. Phys. Rev. 73: 916. 1948.
21. HIRZEL, O. and WÄFFLER, H. Phys. Rev. 74: 1553. 1948.
22. HOLMES, A. Nature, 159: 127. 1947.
23. HOLMES, A. Nature, 173: 612. 1954.
24. HOUTERMANS, F. G., HAXEL, O., and HEINTZ, J. Z. Physik, 128: 657. 1950.
25. INGHRAM, M. G., BROWN, H., PATTERSON, C., and HESS, D. C. Phys. Rev. 80: 916. 1950.
26. JOHNSON, W. H. Phys. Rev. 88: 1213. 1952.
27. KAHN, B. and LYON, W. S. Phys. Rev. 91: 1212. 1953.

28. KÖHLHORSTER, W. Z. Geophysik, 6: 341. 1930.
29. LINDGREN, W. Mineral deposits. McGraw-Hill Book Company, Inc., New York. 1948. p. 316.
30. MORRISON, P. Phys. Rev. 82: 209. 1951.
31. MOUSUF, A. K. Phys. Rev. 88: 150. 1952.
32. MÜHLHOFF, A. Ann. Physik, 7: 205. 1930.
33. NIER, A. O. Phys. Rev. 55: 150. 1939; 60: 112. 1941.
34. NIER, A. O. Phys. Rev. 77: 789. 1950.
35. REUTERSWÄRD, C. Arkiv Fysik, 4: 203. 1951.
36. RUSSELL, R. D., FARQUHAR, R. M., CUMMING, G. L., and WILSON, J. T. Trans. Am. Geophys. Union, 35: 301. 1954.
37. RUSSELL, R. D., SHILLIBEER, H. A., FARQUHAR, R. M., and MOUSUF, A. K. Phys. Rev. 91: 1223. 1953.
38. SAWYER, G. A. and WIEDENBECK, M. L. Phys. Rev. 76: 1535. 1949.
39. SAWYER, G. A. and WIEDENBECK, M. L. Phys. Rev. 79: 490. 1950.
40. SHILLIBEER, H. A., RUSSELL, R. D., FARQUHAR, R. M., and JONES, E. A. W. Phys. Rev. 94: 1793. 1954.
41. SMALLER, B., MAY, J., and FREEDMAN, M. Phys. Rev. 79: 940. 1950.
42. SMITS, F. and GENTNER, W. Geochim. et Cosmochim. Acta, 1: 22. 1950.
43. SPIERS, F. W. Nature, 165: 356. 1950.
44. STOUT, R. W. Phys. Rev. 75: 1107. 1949.
45. SUESS, H. E., HAYDEN, R. J., and INGHRAM, M. G. Nature, 168: 432. 1951.
46. THOMSON, J. J. Phil. Mag. 10: 584. 1905. CAMPBELL, N. R. and WOOD, A. Proc. Cambridge Phil. Soc. 14: 15. 1907. CAMPBELL, N. R. Proc. Cambridge Phil. Soc. 14: 211. 1907.
47. THOMPSON, F. C. and ROWLANDS, S. Nature, 152: 103. 1943.
48. WASSERBURG, G. J. and HAYDEN, R. J. Phys. Rev. 93: 645. 1954.

H-PLANE BIFURCATION OF RECTANGULAR WAVEGUIDES[1]

By R. A. Hurd and H. Gruenberg

ABSTRACT

Using a method based on the calculus of residues, a rigorous solution has been obtained for the problem of the bifurcation of a rectangular waveguide. Expressions are given for the amplitudes of all the reflected and transmitted modes in the guide. A comparison is made with results obtained by the transform method of Wiener and Hopf.

INTRODUCTION

In the solution of electromagnetic boundary value problems of all but the most trivial type, infinite sets of equations in an infinity of unknowns may arise. The solution of such sets is often very difficult, and usually approximate methods have to be resorted to. However, in recent years a technique for the exact solution of a certain class of these equations has been developed (1, 3, 6, 7). This method, which is based upon the calculus of residues in the theory of the complex integral calculus, seems to offer a powerful tool for the solution of many such problems.

The problem to be considered here is the bifurcation of a rectangular guide by a semi-infinite septum parallel to the electric vector of the incident TE_{10}-modes. This problem has been solved rigorously by the Wiener–Hopf method (4). The method used here makes use of the calculus of residues and is somewhat simpler and more straightforward.

STATEMENT OF THE PROBLEM

The configuration to be studied is shown in Fig. 1. A rectangular guide of width a is fitted with a perfectly conducting, infinitely thin septum starting

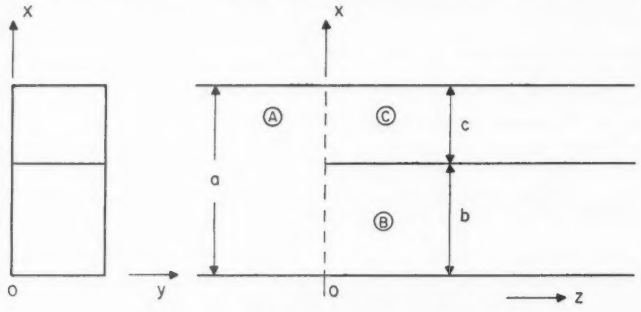

Fig. 1. *H*-plane bifurcation of waveguide.

from some reference plane ($z = 0$) and extending to infinity towards the right. For the purpose of analysis the space inside the guide will be divided into

[1]*Manuscript received July 14, 1954.*
Contribution of the Radio and Electrical Engineering Division, National Research Council, Ottawa, Canada. Issued as N.R.C. No. 3399.

three subregions (see Fig. 1): subregion A represents the space inside the main guide for $z < 0$, subregions B and C represent the spaces in the two branches for $z > 0$.

It is assumed that a TE_{10}-mode with the electric vector parallel to the edge of the septum is incident on the plane $z = 0$ from each of the three subregions. (This assumption is somewhat more general than is usually necessary in practice.) A system of reflected modes will be set up in the three regions, with amplitudes and phases adjusted to satisfy all boundary conditions. Since the incident fields are independent of the y-coordinate and the entire structure is cylindrical with respect to the y-axis, the total fields in the three regions will also be independent of y. The only field components present will be E_y, H_x, and H_z. The entire field can be derived from a two-dimensional scalar wave function $\phi = E_y$.

The problem, therefore, is to find solutions to the two-dimensional wave equation

$$\frac{\partial^2\phi}{\partial x^2}+\frac{\partial^2\phi}{\partial z^2}+k^2\phi = 0, \tag{1}$$

subject to the following conditions:

(a) ϕ and $\nabla\phi$ are finite in all three subregions, except at the edge of the septum ($z = 0$, $x = b$) where $|\nabla\phi|$ becomes infinite.

(b) ϕ and $\nabla\phi$ are continuous in all three subregions and across the interface at $z = 0$.

(c) ϕ represents outgoing waves at $z = \pm\infty$ apart from the incident components.

(d) ϕ vanishes on the walls $x = 0$, $x = a$; and on the septum.

(e) ϕ goes to zero as $r^{\frac{1}{2}}$ as the edge of the septum is approached (r is the distance from the edge). This implies that $|\nabla\phi|$ (i.e. the magnetic field) goes to infinity as $r^{-\frac{1}{2}}$ at the edge (2, 5).

ANALYSIS

The following wave functions satisfy conditions (a), (c), and (d) in regions A, B, and C, respectively:

$$\begin{aligned}
\phi_A &= A\sin\frac{\pi x}{a}e^{-\alpha_1 z}+\sum_{n=1}^{\infty}A_n\sin\frac{n\pi x}{a}e^{\alpha_n z},\\
\phi_B &= B\sin\frac{\pi x}{b}e^{\beta_1 z}+\sum_{n=1}^{\infty}B_n\sin\frac{n\pi x}{b}e^{-\beta_n z},\\
\phi_C &= C\sin\frac{\pi(x-b)}{c}e^{\gamma_1 z}+\sum_{n=1}^{\infty}C_n\sin\frac{n\pi(x-b)}{c}e^{-\gamma_n z}.
\end{aligned} \tag{2}$$

The first term in each expression represents the incident fields, and the α_n, β_n, and γ_n are the propagation constants in the three regions. They are given by

$$\begin{aligned}
\alpha_n &= [(n\pi/a)^2-k^2]^{\frac{1}{2}},\\
\beta_n &= [(n\pi/b)^2-k^2]^{\frac{1}{2}},\\
\gamma_n &= [(n\pi/c)^2-k^2]^{\frac{1}{2}},
\end{aligned} \tag{3}$$

where $k = 2\pi/\lambda$ is the phase constant for free space.* In most practical cases, where $\lambda/2 < a < \lambda$, all propagation constants will be real except for α_1 and perhaps β_1 *or* γ_1. Hence, one mode only can propagate in region A, and one mode *may* propagate in region B *or* C but not in both. One of the amplitudes B or C, or both, will usually be zero.

Continuity of the tangential field components across the interface $z = 0$ (condition (b)) requires that

$$[4a] \quad \sum_{n=1}^{\infty} (A\delta_n^1 + A_n) \sin\frac{n\pi x}{a} = \sum_{p=1}^{\infty} (B\delta_p^1 + B_p) \sin\frac{p\pi x}{b} \quad \text{for } 0 < x < b,$$

$$= \sum_{p=1}^{\infty} (C\delta_p^1 + C_p) \sin\frac{p\pi(x-b)}{c} \quad \text{for } b < x < a,$$

$$[4b] \quad \sum_{n=1}^{\infty} \alpha_n(-A\delta_n^1 + A_n) \sin\frac{n\pi x}{a} = \sum_{p=1}^{\infty} \beta_p(B\delta_p^1 - B_p) \sin\frac{p\pi x}{b} \quad \text{for } 0 < x < b,$$

$$= \sum_{p=1}^{\infty} \gamma_p(C\delta_p^1 - C_p) \sin\frac{p\pi(x-b)}{c} \quad \text{for } b < x < a,$$

where

$$[5] \quad \delta_n^1 = \begin{cases} 0 & \text{for } n \neq 1 \\ 1 & \text{for } n = 1 \end{cases}.$$

One may consider the expressions on the right as Fourier sine series representing periodic functions of period b and c, respectively, which are equal to the left-hand sides in the range $0 < x < b$ and $b < x < a$, respectively. The coefficients in these sine series are determined in the usual manner:

$$[6a] \quad B\delta_p^1 + B_p = (-)^p \frac{2p\pi}{b^2} \sum_{n=1}^{\infty} (A\delta_n^1 + A_n) \frac{\sin(n\pi b/a)}{\alpha_n^2 - \beta_p^2},$$

$$[6b] \quad C\delta_p^1 + C_p = -\frac{2p\pi}{c^2} \sum_{n=1}^{\infty} (A\delta_n^1 + A_n) \frac{\sin(n\pi b/a)}{\alpha_n^2 - \gamma_p^2},$$

$$[6c] \quad \beta_p(Bo_p^1 - B_p) = (-)^p \frac{2p\pi}{b^2} \sum_{n=1}^{\infty} \alpha_n(-A\delta_n^1 + A_n) \frac{\sin(n\pi b/a)}{\alpha_n^2 - \beta_p^2},$$

$$[6d] \quad \gamma_p(C\delta_p^1 - C_p) = -\frac{2p\pi}{c^2} \sum_{n=1}^{\infty} \alpha_n(-A\delta_n^1 + A_n) \frac{\sin(n\pi b/a)}{\alpha_n^2 - \gamma_p^2}.$$

It is to be noted that the series [4b] are not absolutely convergent, since the coefficients A_n, B_p, C_p, as will be seen later, behave as $n^{-3/2}$ for large n. The validity of the term-by-term integration involved in obtaining the Fourier coefficients may therefore be questioned.

It is possible, however, to show that Equations [6] are correct. Green's second identity,

$$\oint \left(\varphi \frac{\partial G}{\partial n} - G \frac{\partial \varphi}{\partial n}\right) ds = 0,$$

*Time dependence $e^{j\omega t}$ is assumed.

is applied to the contour *DEFGHJD* in Fig. 2. G is chosen to be successively

$$G = \sin(p\pi x/a)\sin\beta_p(z+\delta),$$

$$G = \sin(p\pi x/a)\cos\beta_p(z+\delta),$$

($p = 1, 2, 3, \ldots$). Along JD and EF the integrations vanish automatically while the contributions from FG and GH vanish when the radius of the

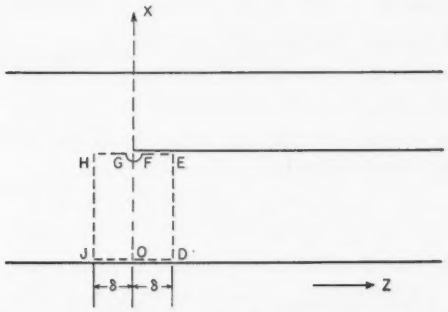

FIG. 2. Contour of integration.

semicircle FG and δ tend to zero. The integrations along DE, HJ involve only the absolutely converging series in Equations [2], and yield Equations [6*a*] and [6*c*] in the limit $\delta = 0$. A similar argument leads to Equations [6*b*] and [6*d*].

In deriving Equations [6], it has been assumed that b/a is not rational. When b/a is rational, some terms of the series will become indeterminate. It is easily seen, however, that Equations [6] and all the following equations (including the final results) are still correct, if these indeterminate terms are replaced by their limits as a/b approaches a rational number.

When B_p and C_p are eliminated from Equations [6], two sets of equations are obtained for the coefficients A_n, viz.:

$$[7] \qquad \begin{aligned} \sum_{n=1}^{\infty} \frac{A_n \sin(n\pi b/a)}{\alpha_n - \beta_p} - \frac{A \sin(\pi b/a)}{\alpha_1 + \beta_p} + \frac{b^2\beta_1}{\pi} B\delta_p^1 &= 0, \\ \sum_{n=1}^{\infty} \frac{A_n \sin(n\pi b/a)}{\alpha_n - \gamma_p} - \frac{A \sin(\pi b/a)}{\alpha_1 + \gamma_p} + \frac{c^2\gamma_1}{\pi} C\delta_p^1 &= 0. \end{aligned}$$

Solutions must be found for the A_n which satisfy Equations [7] simultaneously and which lead to fields that satisfy the edge condition (*e*) of the first section.

Similarly, when B and C are eliminated from Equations [6] one obtains

$$[8] \qquad \begin{aligned} (-)^p \frac{b^2\beta_p B_p}{p\pi} &= \frac{A \sin(\pi b/a)}{\alpha_n - \beta_p} - \sum_{n=1}^{\infty} \frac{A_n \sin(n\pi b/a)}{\alpha_n + \beta_p}, \\ -\frac{c^2\gamma_p C_p}{p\pi} &= \frac{A \sin(\pi b/a)}{\alpha_n - \gamma_p} - \sum_{n=1}^{\infty} \frac{A_n \sin(n\pi b/a)}{\alpha_n + \gamma_p}. \end{aligned}$$

SOLUTION OF THE EQUATIONS

Consider a function $f(w)$ of a complex variable which is analytic except for simple poles at $w = \alpha_n$ $(n = 1, 2, 3, \ldots)$ and at $w = -\alpha_1$. Assume also that $f(w)$ has zeros at $w = \beta_n$ and $w = \gamma_n$ $(n = 2, 3, \ldots)$. If contours C_s are chosen to enclose the pole at $w = -\alpha_1$ and the poles at $w = \alpha_n$, $n \leqslant s$ only, then by Cauchy's theorem,

$$[9] \qquad \begin{aligned} \frac{1}{2\pi j}\int_{C_s}\frac{f(w)dw}{w-\beta_p} &= \sum_{n=1}^{s}\frac{r(\alpha_n)}{\alpha_n-\beta_p}-\frac{r(-\alpha_1)}{\alpha_1+\beta_p}+f(\beta_1)\delta_p^1, \\ \frac{1}{2\pi j}\int_{C_s}\frac{f(w)dw}{w-\gamma_p} &= \sum_{n=1}^{s}\frac{r(\alpha_n)}{\alpha_n-\gamma_p}-\frac{r(-\alpha_1)}{\alpha_1+\gamma_p}+f(\gamma_1)\delta_p^1, \end{aligned}$$

where $r(\alpha_n)$ is the residue of $f(w)$ at $w = \alpha_n$.

If $f(w)$ can be selected so that the integrals on the left tend to zero as $s \to \infty$ and if $f(w)$ is normalized to make

$$[10] \qquad \begin{aligned} r(-\alpha_1) &= A\sin(\pi b/a), \\ f(\beta_1) &= b^2\beta_1 B/\pi, \\ f(\gamma_1) &= c^2\gamma_1 C/\pi, \end{aligned}$$

then Equations [8] become formally identical with [7] and one obtains

$$[11] \qquad A_n = r(\alpha_n)\operatorname{cosec}(n\pi b/a).$$

The vanishing of the contour integrals in [9] as $s \to \infty$ is equivalent to the condition that $f(w) \to 0$ as $|w| \to \infty$ if the neighborhoods of the poles of $f(w)$ are excluded.

To find explicit expressions for B_p and C_p one starts with the contour integrals

$$[12] \qquad \begin{aligned} \frac{1}{2\pi j}\int_{C_s}\frac{f(w)dw}{w+\beta_p} &= \sum_{n=1}^{s}\frac{r(\alpha_n)}{\alpha_n+\beta_p}-\frac{r(-\alpha_1)}{\alpha_1-\beta_p}+f(-\beta_p), \\ \frac{1}{2\pi j}\int_{C_s}\frac{f(w)dw}{w+\gamma_p} &= \sum_{n=1}^{s}\frac{r(\alpha_n)}{\alpha_n+\gamma_p}-\frac{r(-\alpha_1)}{\alpha_1-\gamma_p}+f(-\gamma_p). \end{aligned}$$

These contour integrals vanish as $s \to \infty$. Because of [10] and [11], Equations [12] are then equivalent to Equations [8] if one sets

$$[13] \qquad \begin{aligned} B_p &= (-)^p(p\pi/b^2\beta_p)f(-\beta_p), \\ C_p &= -(p\pi/c^2\gamma_p)f(-\gamma_p). \end{aligned}$$

It is seen that once the function $f(w)$ is known, the coefficients A_n, B_n, and C_n can be found explicitly from [11] and [13]. To obtain the right poles and zeros, $f(w)$ must have the form

$$[14] \qquad f(w) = g(w)\frac{\Pi(w,\beta)\,\Pi(w,\gamma)}{(w+\alpha_1)(w-\beta_1)(w-\gamma_1)\,\Pi(w,\alpha)}$$

where $g(w)$ is an entire function, $\Pi(w, \alpha)$ is the infinite product

$$[15] \qquad \Pi(w,\alpha) = \prod_{p=1}^{\infty}(\alpha_p-w)(a/p\pi)\,e^{aw/p\pi},$$

and $\Pi(w, \beta)$ and $\Pi(w, \gamma)$ are similar infinite products with β and γ replacing α, and b and c replacing a. The factors $(a/p\pi)$ and the exponential factors have been introduced to make the products absolutely and uniformly convergent.

The asymptotic behavior of $f(w)$ as $|w| \to \infty$ can be investigated in a manner similar to that used by Whitehead (7). It is found that

$$[16] \quad f(w) \sim (-a/2bcw^7)^{\frac{1}{2}} g(w) \exp[-(bw/\pi)\ln(a/b) - (cw/\pi)\ln(a/c)]$$

for $0 < \arg w < 2\pi$, and

$$[17] \quad f(w) \sim \left(\frac{2a}{bcw^7}\right)^{\frac{1}{2}} g(w) \frac{\sin b(w^2+k^2)^{\frac{1}{2}} \sin c(w^2+k^2)^{\frac{1}{2}}}{\sin a(w^2+k^2)^{\frac{1}{2}}} \times \exp[-(bw/\pi)\ln(a/b) - (cw/\pi)\ln(a/c)],$$

in the neighborhood of the positive real axis. To ensure that $f(w) \to 0$ as $|w| \to \infty$ in both halves of the w-plane, excluding the neighborhood of the poles of $f(w)$, $g(w)$ must be of the form

$$[18] \quad g(w) = P(w) \exp[(bw/\pi)\ln(a/b) + (cw/\pi)\ln(a/c)],$$

where $P(w)$ is a polynomial of, at the most, third degree. It will be shown below that $P(w)$ must, in fact, be a second-degree polynomial so that the only remaining boundary condition, the edge condition (e) of the first section, is satisfied.

The formal solution to the problem is thus given by

$$[19] \quad f(w) = \frac{e_2 w^2 + e_1 w + e_0}{(w+\alpha_1)(w-\beta_1)(w-\gamma_1)} \frac{\Pi(w, \beta)\, \Pi(w, \gamma)}{\Pi(w, \alpha)} \times \exp[(bw/\pi)\ln(a/b) + (cw/\pi)\ln(a/c)],$$

and the Equations [11] and [13]. The coefficients e_0, e_1, and e_2 can be found from the three linear equations obtained by substituting [19] in [10].

The asymptotic behavior as $|w| \to \infty$ is given by

$$[20] \quad f(w) \sim e_2 \left(-\frac{a}{2bcw^3}\right)^{\frac{1}{2}}, \quad \text{for } 0 < \arg w < 2\pi,$$

$$f(w) \sim e_2 \left(\frac{2a}{bcw^3}\right)^{\frac{1}{2}} \frac{\sin b(w^2+k^2)^{\frac{1}{2}} \sin c(w^2+k^2)^{\frac{1}{2}}}{\sin a(w^2+k^2)^{\frac{1}{2}}}, \quad \text{for } \arg w = 0.$$

The second expression gives the correct poles and zeros on the positive real axis.

INVESTIGATION OF THE EDGE CONDITION

To establish that the above solution is unique, it is necessary to show that the electric field ϕ goes to zero as $r^{\frac{1}{2}}$ or that the magnetic field $|\nabla\phi|$ goes to infinity as $r^{-\frac{1}{2}}$ as the edge of the septum is approached. The second condition is easier to verify. It is equivalent to the requirement that the current density on the septum, which is proportional to $\partial\phi/\partial x$, go to infinity as $r^{-\frac{1}{2}}$ near the edge.

From [2] and [13] the current density on the side of the septum ($z > 0$, $x = b$) facing region B is proportional to

[21] $$\left(\frac{\partial\phi}{\partial x}\right)_{x=b} = -B\frac{\pi}{b}e^{\beta_1 z} + \sum_1^\infty \left(\frac{n\pi}{b}\right)^2 \frac{f(-\beta_n)}{\beta_n b} e^{-\beta_n z}.$$

For large values of n, $\beta_n \sim n\pi/b$ and $f(-\beta_n) \sim (n\pi/b)^{-3/2}$. Hence the above series differs by only a bounded function of z from the series

[22] $$S = K\sum_{n=1}^{\infty} n^{-\frac{1}{2}} e^{-n\pi z/b},$$

where K is a constant. It is easily seen that S behaves like $z^{-\frac{1}{2}}$ as z tends to zero by considering the inequality

[23] $$\int_1^\infty \frac{e^{-\xi u}}{u^{\frac{1}{2}}}\,du \leqslant \sum_{n=1}^{\infty} \frac{e^{-n\xi}}{n^{\frac{1}{2}}} \leqslant \int_0^\infty \frac{e^{-\xi u}}{u^{\frac{1}{2}}}.$$

The integral on the right is $(\pi/\xi)^{\frac{1}{2}}$, the one on the left is $(\pi/\xi)^{\frac{1}{2}} - 2 + 2\xi/3 \ldots$ which also tends to $(\pi/\xi)^{\frac{1}{2}}$ as $\xi \to 0$.

The proof for the current density on the other side of the septum is exactly analogous. Similarly, one can show that $H_z \propto \partial\phi_A/\partial z$ has the correct singularity at the edge when the approach is made from region A. In this case, the residues $r(\alpha_n)$ for large n are found from the second expression in [20]:

[24] $$r(\alpha_n) \sim -e_2(2/abc)^{\frac{1}{2}}(n\pi/a)^{-3/2}\sin^2(n\pi b/a).$$

From [2] and [11] it is then seen that H_x differs by only a bounded function of x and z from the series

[25] $$S' = K'\sum_1^\infty n^{-\frac{1}{2}} e^{n\pi z/a}\sin(n\pi b/a)\sin(n\pi x/a), \quad z < 0,$$

$$= K'\sum_1^\infty n^{-\frac{1}{2}} e^{-n\pi z'/a}\sin(n\pi b/a)\sin(n\pi\{b+\rho z'\}/a),$$

where $z' = |z|$, $x = b + x' = b + \rho z'$. As $z' \to 0$, this series can be shown to be of order $(z')^{-\frac{1}{2}}$ by a method similar to that used in Reference (3).

DISCUSSION OF SPECIFIC CASES

In practice the guide dimensions will be such that α_1 is purely imaginary (say $\alpha_1 = j2\pi/\lambda_A$, where λ_A is the guide wavelength of the TE_{10}-mode in region A) but all other α's are real. One may then assume without loss of generality that all the β's for $n > 1$ and all the γ's are real. Only two cases need to be considered: (I) β_1 is real, and (II) β_1 is imaginary ($\beta_1 = j2\pi/\lambda_B$, where λ_B is the guide wavelength in B).

It will be assumed that a TE_{10}-mode of unit amplitude is incident from region A, but no waves are incident from the right ($A = 1$, $B = C = 0$). From [10] and [19] one obtains

[26] $$f(w) = \frac{\sin(\pi b/a)}{w+\alpha_1}\,\frac{\Pi(w,\beta)\,\Pi(w,\gamma)}{\Pi(-\alpha_1,\beta)\,\Pi(-\alpha_1,\gamma)}\,\frac{\Pi(-\alpha_1,\alpha)}{\Pi(w,\alpha)} \times \exp[(w+\alpha_1/\pi)\{b\ln(a/b)+c\ln(a/c)\}],$$

and from [11] the reflection coefficient referred to the plane $z = 0$ is

$$[27]\quad R = A_1 = \frac{\Pi^{(1)}(-\alpha_1, \alpha)\,\Pi(\alpha_1, \beta)\,\Pi(\alpha_1, \gamma)}{\Pi^{(1)}(\alpha_1, \alpha)\,\Pi(-\alpha_1, \beta)\,\Pi(-\alpha_1, \gamma)} \times \exp[(2\alpha_1/\pi)\{-a+b\ln(a/b)+c\ln(a/c)\}],$$

where the bracketed superscript on the product sign means that the factor $n = 1$ is to be omitted from the product. Note that $\alpha_1 = j2\pi/\lambda_A$.

Case I: β_1 is real. From [27] and [15] it is seen that $|R| = 1$, i.e., there is complete reflection, as could be expected from physical reasoning since no waves are propagated in regions B and C. The junction introduces a phase shift equal to

$$[28]\quad \arg R = -2\left[\frac{2a}{\lambda_A}\left(1-\frac{b}{a}\ln\frac{a}{b}-\frac{c}{a}\ln\frac{a}{c}\right)-\dot{S}_2\left(\frac{2a}{\lambda_A};\,1,0\right) +S_1\left(\frac{2b}{\lambda_A};\,\frac{b}{a},\,0\right)+S_1\left(\frac{2c}{\lambda_A};\,\frac{c}{a},\,0\right)\right],$$

where

$$[29]\quad S_N(u;v,0) = \sum_{n=N}^{\infty}\left[\sin^{-1}\frac{u}{(n^2-v^2)^{\frac{1}{2}}}-\frac{u}{n}\right].$$

This is equivalent to removing the septum and placing a short circuit at $z = -\frac{1}{2}\arg R$ in the guide in agreement with the result in the Waveguide Handbook (Ref. 4, p. 174).

Case II: β_1 is purely imaginary. In this case one obtains

$$[30]\quad |R| = \frac{1-\lambda_B/\lambda_A}{1+\lambda_B/\lambda_A},$$

$$[31]\quad \arg R = -2\left\{-\frac{2a}{\lambda_A}\left(\frac{b}{a}\ln\frac{a}{b}+\frac{c}{a}\ln\frac{a}{c}\right)-S_2\left(\frac{2a}{\lambda_A};\,1,0\right) +S_2\left(\frac{2b}{\lambda_A};\,\frac{b}{a},0\right)+S_2\left(\frac{2c}{\lambda_A};\,\frac{c}{a},0\right)+\sin^{-1}\frac{2c/\lambda_A}{[1-(c/a)^2]^{\frac{1}{2}}}\right\}.$$

Similar expressions are obtained when a wave is incident from the right ($A = C = 0, B = 1$). The result can be interpreted in terms of an equivalent circuit and agrees with that given in the Waveguide Handbook (4, p. 305).

REFERENCES

1. Berz, F. Proc. Inst. Elec. Engrs. (London), Pt. III, 98: 47. 1951.
2. Bouwkamp, C. J. Physica, 12: 467. 1946.
3. Gruenberg, H. and Hurd, R. A. Natl. Research Council Can. Rept. ERA 268, 1954.
4. Marcuvitz, N. Waveguide Handbook. McGraw-Hill Book Company, Inc., New York. 1951.
5. Meixner, J. Ann. Physik, 6: 1. 1949.
6. Szekely, Z. M.A.Sc. Thesis, University of Toronto, Toronto, Ont. 1953.
7. Whitehead, E. A. N. Proc. Inst. Elec. Engrs. (London), Pt. III, 98: 133. 1951.

A METHOD OF CONCENTRATING He^3–He^4 MIXTURES[1]

By K. R. Atkins[2] and D. R. Lovejoy[3]

ABSTRACT

We have developed a method of increasing the concentration of He^3 in He^3–He^4 mixtures by "superfluid filtration", relying upon the fact that liquid He^4 flows rapidly through a small leak while the He^3 in solution remains behind. In this way an increase in concentration from 2% to 95% can be achieved in a single operation. The rate of processing is about 200 standard cc. of the initial gaseous mixture per hour.

1. INTRODUCTION

Enrichment of the He^3 content of He^3–He^4 mixtures has been achieved by the conventional methods of thermal diffusion (2, 13, 15, 16) and fractional distillation (7). However, the failure of liquid He^3 to become superfluid like liquid He^4 suggested entirely new methods. The method of "superfluid filtration" (5, 6) was based on the observation that liquid He^4 flows rapidly through a narrow channel, while liquid He^3 does not. The "heat flush" method (7, 11, 14, 17, 19) took advantage of the fact that the He^3 moves with the normal component of the liquid He^4 away from a source of heat.

In most of these investigations, however, the initial mixture was either atmospheric helium containing 1 part in 10^6 of He^3, or well helium containing about 1 part in 10^7 of He^3, and the final concentration never exceeded 1.5%. In one case (14) the thermal diffusion method was first used to obtain a concentration of 0.01% and the heat flush method was then applied to achieve a final concentration of 4%. The work described in the present paper started with mixtures produced as a by-product of the operation of the Chalk River nuclear reactor, which contained between 2% and 4% of He^3. Our task was to raise the concentration to at least 25% in order that the mixtures might be useful for nuclear bombardment experiments, and we also hoped that we might achieve still higher concentrations because of the interest attached to the properties of these mixtures in the liquid state. We chose the method of superfluid filtration because Abraham, Weinstock, and Osborne (1), in the course of their work on the λ-points of He^3–He^4 mixtures, had obtained appreciable enrichment by this method in the concentration range that interested us. In practice the method proved simple and effective, and we were able to develop it to the point of obtaining a concentration of 95% after a single filtration.

A short preliminary account of the earlier stages of this work has already been published (3). A detailed account has been given in the Ph.D. thesis of D. R. Lovejoy (12).

Throughout this paper, percentage concentration is defined as $100\ N_3/(N_3+N_4)$, where N_3 and N_4 are the numbers of gram moles of He^3 and He^4 present.

[1]*Manuscript received July 27, 1954.*
Contribution from the Department of Physics, University of Toronto, Toronto, Ont.
[2]*Now at: Department of Physics, University of Pennsylvania, Philadelphia, Penn.*
[3]*Now at: National Research Council Laboratories, Ottawa, Canada.*

2. APPARATUS AND METHOD

The apparatus is shown diagrammatically in Fig. 1. The superleak L was of the type originally used by Giauque, Stout, and Barieau (9), and was made by sealing a 7 cm. length of 0.18 mm. diameter platinum wire into pyrex glass. Upon cooling to low temperatures the platinum shrank away

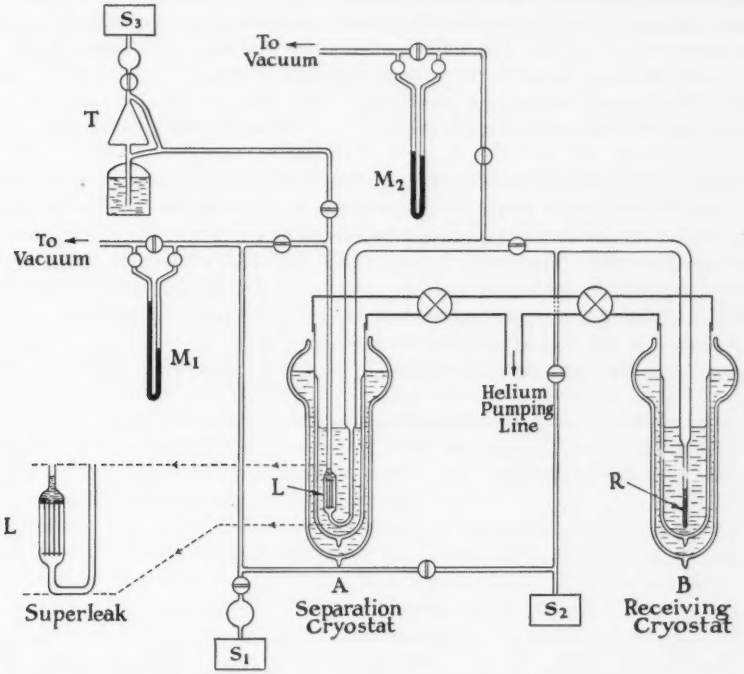

FIG. 1. The apparatus.

from the glass, leaving a gap which was found to have a mean width of about 10^{-4} cm. by observing the rate of flow of helium gas through it at liquid helium temperatures. In the final apparatus 10 such superleaks were used in parallel. The platinum wire was wound lengthwise on a short length of pyrex tube which was then placed inside another pyrex tube, filled with a pyrex rod, and the whole assembly melted down and drawn out.

A measured quantity of low concentration mixture from the container S_1 was liquefied on top of the superleak, which was immersed in a liquid helium bath at 1.3°K. Flow through the leak started immediately, but ceased as soon as the pressure on the exit side became comparable with the saturated vapor pressure. The explanation of this may be that the liquid mixture on the exit side had a lower concentration than on the entrance side, and the resulting osmotic pressure (4, 20) was large enough to prevent flow. When the exit

side was pumped and the pressure there kept below the saturated vapor pressure to prevent the formation of bulk liquid, the flow started again. As the amount of He^3 in the effluent was sufficient to justify its recovery, an ordinary pumping system could not be used, and it was not possible to design a Toepler pump with a high enough speed. The tube from the exit side of the superleak was therefore taken out of the separation cryostat *A* into the receiving cryostat *B*, which was maintained at the slightly lower temperature of 1.1°K. The effluent therefore distilled over from *A* to *B* and collected as a liquid in the tube *R*. Cryostat *B* was equivalent to a pump with a high speed limited only by the diameter of the connecting tube. At the end of the run the impoverished mixture in *R* was boiled off into the container S_2.

Although the liquid flowing through the superleak contained a little He^3, its concentration was much less than in the initial mixture, and so the concentration of He^3 in the liquid left behind at the entrance to the superleak increased steadily. The vapor pressure of a He^3–He^4 mixture increases with increasing He^3 concentration and has been measured up to concentrations of 13% (18). It was therefore possible to follow the course of the enrichment by observing the vapor pressure on the manometer M_1. Curve *A* of Fig. 2 shows that the concentration increased slowly at first, then more rapidly,

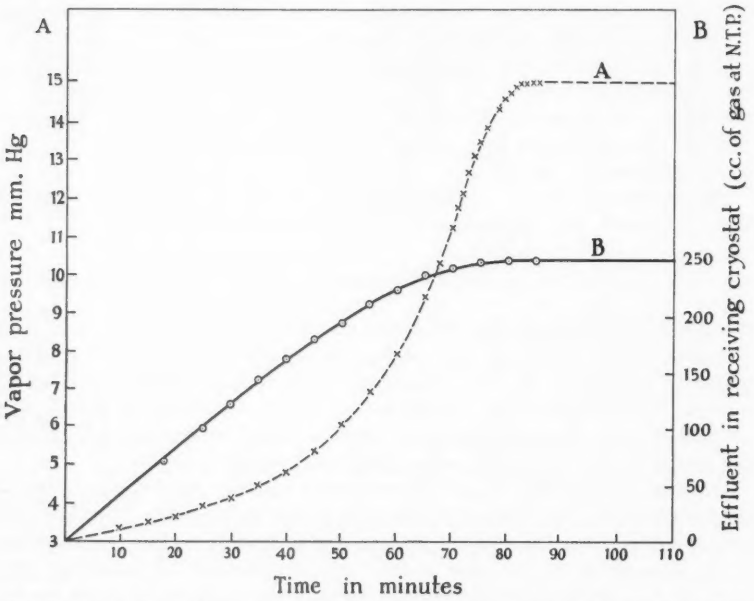

FIG. 2. Curve *A*: the vapor pressure of the liquid at the entrance to the superleak. Curve *B*: the amount of liquid which has passed through the superleak, as deduced from the height of the liquid column in the tube *R*. The initial charge was 250 standard cc. of 2% mixture.

and finally levelled off as the flow came to an end. Curve B shows the amount of liquid which passed through the superleak as a function of time, and was deduced from the level of the liquid in the tube R. The manometer M_2 enabled a check to be kept on the concentration of the effluent.

When the filtration had come to an end and the vapor pressure registered on M_1 had reached its maximum value, the enriched mixture was removed by the Toepler pump T into the container S_3. Its concentration was measured with a mass spectrometer.

3. PERFORMANCE

The maximum vapor pressure attained at the end of a filtration always corresponded to a liquid concentration of $24 \pm 2\%$, but the measured concentration of the enriched mixture was always considerably greater than this. This is easily understood once we realize that the vapor in equilibrium with a 24% liquid mixture has a concentration of about 95% (18), and that the dead space above the superleak at liquid helium temperatures was of the order of 0.75 cm.^{3} and therefore held a considerable mass of vapor. It follows that there is an optimum value for the quantity of gas initially introduced if one wishes to realize the maximum final concentration. If a smaller quantity of gas is introduced, all the liquid flows through the superleak before a liquid concentration of 24% is reached. If a larger quantity than the optimum is used, then liquid remains at the end of the filtration and lowers the mean concentration below that of the vapor. For our apparatus, we determined experimentally that this optimum quantity was 200 standard cc. of 2% mixture or 100 standard cc. of 4% mixture.

However, even when this optimum initial charge was used, the resulting mean concentration was still not 95% but about 45%. This anomaly was traced to the fact that the gas in the dead space at room temperature had a concentration in the range 2–4%, having experienced no appreciable enrichment. It is not yet clear whether this was because a low concentration mixture at room temperature can remain in equilibrium with a high concentration mixture at liquid helium temperatures, or because the rate of diffusion of He^3 from the low to the high temperature was very slow. The difficulty was surmounted by skimming off the gas at room temperature and then removing the cold gas separately. It was in this way that a final concentration of 95% was achieved. For the procedure which gave this high concentration, the rate of processing was 200 standard cc. of the initial 2% mixture per hour, yielding about 2 standard cc. of 95% mixture per hour. Only 50% of the He^3 in the initial charge was contained in the 95% mixture, 25% having been lost through the superleak and 25% removed with the gas at room temperature which had been skimmed off.

No attempt was made to increase the concentration above 95% by this method. It is probably more feasible to bridge the gap between 95% and 100% by fractional distillation. We have been able to raise the concentration from 80% to 92% merely by liquefying the 80% mixture in a glass capillary at 1.1°K. and pumping off the enriched vapor with a Toepler pump. Starting

with a high concentration mixture, Fairbank, Ard, Dehmelt, Gordy, and Williams (8) have used fractional distillation to produce concentrations better than 99%.

The concentration of the effluent collected in the receiving cryostat depended upon the initial concentration and also the initial charge in a complicated way (12). This impoverished mixture could also be processed and the final concentration was found to be almost independent of the initial concentration. The rate of processing was, in fact, slightly higher, but, of course, the yield in cubic centimeters of high concentration mixture per hour was much less and the procedure became unduly laborious when the initial concentration was less than 0.3%.

The fact that He^3 was able to flow through the superleak should not necessarily be taken as evidence that it can participate in superfluid flow. The possibility of ordinary viscous flow of the He^3 cannot be excluded. The situation may have been complicated by thermal gradients and concentration gradients, and the effective pressure forcing the He^3 through the leak may have been quite large. Moreover, there is some evidence (10) that the effective viscosity of the normal component of He^4 is very small in channels of this width, perhaps because of mean free path effects, and similar considerations may apply to He^3 in solution.

ACKNOWLEDGMENTS

The He^3–He^4 mixtures were provided by Atomic Energy of Canada, Ltd., who also undertook many of the mass spectrometer analyses. The remaining analyses were performed by Drs. C. B. Collins, R. D. Russell, and R. M. Farquhar of the University of Toronto. During the early stages of the work Mr. J. C. Findlay gave invaluable assistance and Prof. A. C. H. Hallett frequently gave helpful advice. The superleaks were made by Mr. H. Chappell. We are particularly grateful to Prof. W. H. Watson who suggested the problem and maintained a helpful interest throughout the research. One of us (D.R.L.) gratefully acknowledges the financial assistance provided by a Garnet W. McKee – Lachlan Gilchrist Scholarship.

REFERENCES

1. Abraham, B. M., Weinstock, B., and Osborne, D. W. Phys. Rev. 76: 864. 1949.
2. Andrew, A. and Smythe, W. R. Phys. Rev. 74: 496. 1948.
3. Atkins, K. R., Findlay, J. C., Lovejoy, D. R., and Watson, W. H. Can. J. Phys. 31: 679. 1953.
4. Daunt, J. G., Probst, R. E., and Johnston, H. L. Phys. Rev. 73: 638. 1948.
5. Daunt, J. G., Probst, R. E., Johnston, H. L., Aldrich, L. T., and Nier, A. O. Phys. Rev. 72: 502. 1947.
6. Daunt, J. G., Probst, R. E., and Nier, A. O. J. Chem. Phys. 15: 759. 1947.
7. Eselson, B. N. and Lazarew, B. G. J. Exptl. Theoret. Phys. (U.S.S.R.), 20: 742. 1950.
8. Fairbank, W. M., Ard, W. B., Dehmelt, H. G., Gordy, W., and Williams, S. R. Phys. Rev. 92: 208. 1953.
9. Giauque, W. F., Stout, J. W., and Barieau, R. E. J. Am. Chem. Soc. 61: 654. 1939.
10. Gorter, C. J. and Mellink, J. H. Physica, 15: 285. 1949.
11. Lane, C. T., Fairbank, H. A., Aldrich, L. T., and Nier, A. O. Phys. Rev. 73: 256. 1948.
12. Lovejoy, D. R. Ph.D. Thesis, University of Toronto, Toronto, Ontario. 1954.
13. McInteer, B. B., Aldrich, L. T., and Nier, A. O. Phys. Rev. 74: 946. 1948.

14. REYNOLDS, C. A., FAIRBANK, H. A., LANE, C. T., MCINTEER, B. B., and NIER, A. O. Phys. Rev. 76: 64. 1949.
15. ROLLIN, B. V. and HATTON, J. Phys. Rev. 74: 508. 1948.
16. SCHUETTE, O. F., ZUCKER, A., and WATSON, W. W. Rev. Sci. Instr. 21: 1016. 1950.
17. SOLLER, T., FAIRBANK, W. M., and CROWELL, A. D. Phys. Rev. 92: 1058. 1953.
18. SOMMERS, H. S. Phys. Rev. 88: 113. 1952.
19. TACONIS, K. W. Ned. Tijdschr. Natuurk. 16: 101. 1950.
20. TACONIS, K. W., BEENAKKER, J. J. M., and DOKOUPIL, Z. Phys. Rev. 78: 171. 1950.

THERMAL EXPANSION OF LITHIUM, 77° TO 300° K.[1]

By W. B. Pearson

ABSTRACT

Measurements of the lattice parameters of lithium at temperatures below 300° K. have been made and the results are compared with previous work and considered in terms of the Grüneisen relationship. Methods of low temperature X-ray photography are also discussed.

INTRODUCTION

Accurate measurement of expansion coefficients at very low temperatures, say 4–80° K., is a matter of some difficulty and at present not many data are available, although there is considerable interest in studying the validity of the Grüneisen relationship at low temperatures (see, for instance, Bijl and Pullan (5)), and in obtaining the expansion coefficients of the inert gases. X-ray cameras have been built in this laboratory to measure accurately lattice parameters at low temperatures and in particular to obtain the expansion coefficients of the alkali metals as part of a general program carried out towards an understanding of the electronic nature of these 'simple' metals.

The present paper describes lattice parameter measurements of lithium in the temperature range 77–300° K. and discusses methods used in low temperature X-ray photography in this laboratory.

LOW TEMPERATURE X-RAY METHODS

The camera used in this investigation between 80° and 300° K. consists of a collimator system and base plate on which a film cassette is precisely located, an adjustable specimen mount, and a synchronous motor for rotating the specimen. The X-ray film is held in a 19 cm. Unicam high temperature camera film cassette as first employed by Basinski and Christian (4). The camera can be used either with the Post, Schwartz, and Fankuchen (17) or Hume-Rothery and Strawbridge (8) method of cooling, while temperatures of 77° or 90° K. can be obtained by running liquid nitrogen or oxygen over the specimen after the method of Smith and Lonsdale (12). The specimen in its adjustable holder may be either hung or supported rampant, being rotated in a bearing accordingly either above or below the X-ray beam.

A method suggested by Dr. J. S. Dugdale has also been used. The X-ray camera is placed in a large cylindrical can having cellophane windows for entry and exit of the X-ray beam, Fig. 1. Although specimen icing is effectively prevented by this method, it suffers from the difficulty that the camera cassette cools somewhat below the temperature at which its dimensions have been measured. Trouble may consequently result through differential contraction of the aluminum alloy film cassette and the steel knife edges. This may change the standard angle θ_k* between the high angle knife edges and

[1]*Manuscript received July 7, 1954.*
Contribution from the Division of Physics, National Research Council, Ottawa, Canada. Issued as N.R.C. No. 3413.
**Notation as used by Lipson and Wilson (10).*

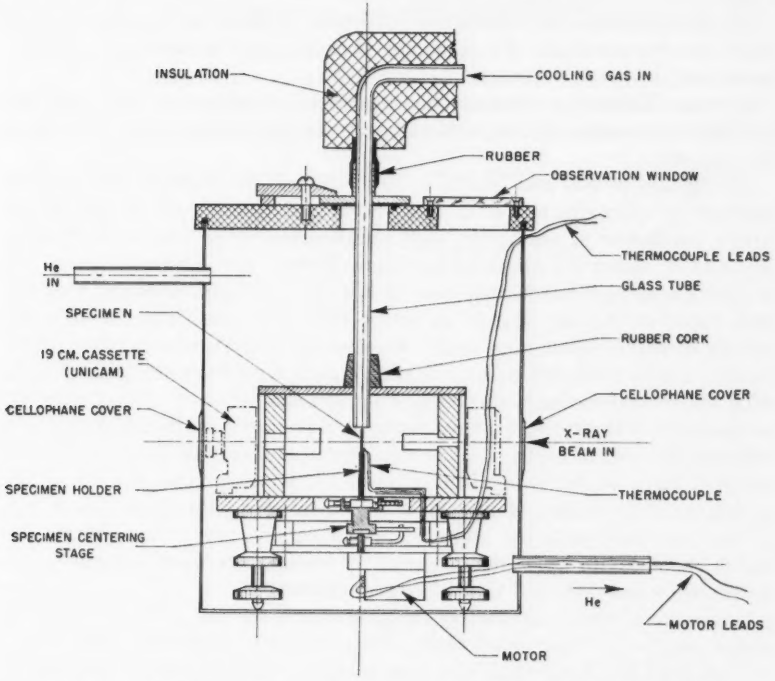

FIG. 1. An arrangement for taking low temperature X-ray powder photographs.

also the standard circumferential distance k between the low angle knife edges. Variation of k is not normally allowed for in taking account of film shrinkage but Lipson and Wilson (10) have shown that the errors involved are negligibly small. Changes of θ_k might indeed be expected to lead to inaccuracies in lattice parameter determination. However, calculations embracing both changes in θ_k and k relative to camera diameter show that the error in the extrapolated lattice parameter obtained from reflections at high Bragg angles is negligibly small for any probable degree of cooling of the film holder—especially in relation to the uncertainties involved in precise determination of specimen temperature.

In order to measure the temperature at which photographs are made, a chromel–alumel or copper–constantan thermocouple has been located so as to touch the specimen just below the level of the X-ray beam. This thermocouple may either be calibrated at fixed points, or *in situ* by measuring the lattice parameter of a substance whose contraction is already well known in the relevant temperature range. The second method is preferable for a number of reasons, among which we may mention:

(1) Calibration of the thermocouple takes place under the exact temperature gradients obtaining in an exposure at any particular temperature.

(2) Any number of exposures and subsequent calibration may be made to relate the characteristics of a particular thermocouple to the standard e.m.f. tables used.

(3) Any differences between thermocouple temperature and effective specimen temperature at the particular temperature of the exposure are taken into account.

$\Delta l/l_0$ values of Nix and MacNair (16) obtained for 99.99% aluminum at intervals of approximately 8° C. have been used to calculate the change of lattice parameter of aluminum with temperature. (The few earlier values obtained by Ebert (7) and used by Hume-Rothery and Strawbridge (8) are in approximate agreement with those of Nix and MacNair.) Calculations have been based on a value of 4.0413_6 kX at 25° C. obtained with an annealed powder of 99.99% aluminum kindly supplied by The Aluminum Company of Canada Limited. In this way calibration curves have been established while using the various methods of cooling. To guard against errors arising from the temperature calibrations, we have made measurements on lithium using two different methods of cooling: (1) the arrangement shown in Fig. 1, and (2) a modified form of the Hume-Rothery and Strawbridge type of cooler. The agreement of both sets of measurements, after using the temperature corrections obtained from the appropriate calibration curves, is certainly well within the absolute experimental errors of temperature measurement, which are probably less than ±4° C. in the range 120–280° K.

In this work lattice parameters are given in kX for ready comparison with earlier work. We have used CuK_α radiation for all photographs ($\lambda_{CuK_{\alpha 1}} = 1.537395$ kX). X-ray films have been measured with a Cambridge universal measuring machine using low magnification, and lattice parameters have been calculated using the Nelson and Riley (15) extrapolation function, applied to resolved doublets occurring at high Bragg angles. The lithium (240) $CuK_{\alpha 1}$ reflection occurs at ~79° to ~81.5°θ and (240) $CuK_{\alpha 2}$ at ~80° to ~82°θ. Lattice parameter measurements are accurate to ±0.0002 kX for the best films and perhaps ±0.0004 kX for the remainder. Combined with an absolute temperature uncertainty of say ±4° C. as mentioned above (1° C. ≡ 0.00016 kX expansion for lithium at room temperature) it is encouraging to find the results of two series of experiments by different methods to be self-consistent to ±0.0002 kX over the whole range.

The lithium used was special sodium-free metal prepared by New Metals and Alloys Limited and used by Kelly and MacDonald (9) for resistance measurements and by MacDonald and Pearson (13) for measurement of thermoelectric force. The residual resistance of the metal, $R_{4.2°K.}/R_{273.2°K.} = 1.5 \times 10^{-3}$, and spectroscopic analysis of the actual X-ray specimens used shows the presence of calcium and very slight traces of sodium as the only metallic impurities. In order to prepare X-ray specimens, the metal was extruded into vaseline to prevent oxidation and lengths were sealed in thin-walled pyrex capillaries which were evacuated. The metal was annealed either at 100° C., or for a long time at room temperature. Several specimens were prepared. One of these used in the range 140–300° K. showed considerable surface discoloration.

RESULTS AND DISCUSSION

In Fig. 2 are shown the lattice parameters of two specimens measured by different techniques in the range 125–300° K., together with that of another specimen measured at 77.5° K. A lattice parameter of 3.5016 kX, corrected to 20° C., is obtained for lithium. This is lower than the value of 3.5023 kX

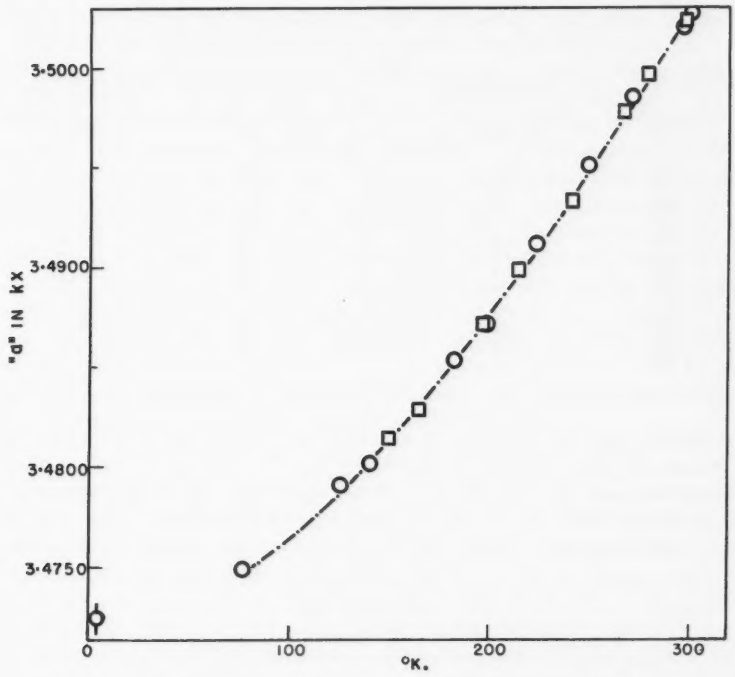

FIG. 2. Low temperature variation of lithium lattice parameters 'a'.
○□ measured values of 'a' using two different methods of cooling.
—·— calculated variation of 'a' with T. (See Text.)

found by Lonsdale and Hume-Rothery (11), but agrees with the estimate of 3.5015 to 3.5019 kX for pure sodium-free lithium made by Aruja and Perlitz (1). The difference of the present result and that of Lonsdale and Hume-Rothery, which lies at the limit of the probable experimental errors, appears to be due to difference in purity of the lithium samples.*

Lonsdale and Hume-Rothery measured the lattice parameter of lithium at 90° K., and the observed contraction to this temperature, $\Delta a_{293\text{-}90°K.} = 0.0261$ kX, agrees with the present findings, $\Delta a_{293\text{-}90°K.} = 0.0258$ kX, to a measurement of one part in ~12,000, which is satisfactory. Only approximate agreement is found with the results of macroscopic measurements made by Simon

**Resistivity measurements and spectroscopic analysis show that the lithium used in this investigation is virtually sodium free. Less than 0.1% sodium in solid solution in the lithium used by Lonsdale and Hume-Rothery would account for the parameter difference.*

and Bergmann (18). It is also noted that the expansion coefficients of copper, iron, and nickel, determined by Simon and Bergmann by the same method as used for lithium and reported in the same paper, are not in agreement with subsequent work, e.g., see comments in Nix and MacNair (16).

The present measurements may be further assessed in terms of the Grüneisen relationship $\alpha = \beta C_v \gamma / 3V$. The temperature variation of the linear thermal expansion coefficient α shown in Table I is obtained for an assumed value of

TABLE I

Temperature, ° K.	Calculated linear expansion coefficient α	Temperature, ° K.	Calculated linear expansion coefficient α
300	46.8	180	36.8
290	46.4	170	35.6
280	45.7	160	34.4
270	45.0	150	33.0
260	44.3	140	31.4
250	43.5	130	29.6
240	42.7	120	27.7
230	41.8	110	25.4
220	40.9	100	23.0
210	40.0	90	20.1
200	39.0	80	17.3
190	38.0		

$\gamma = 0.92$ by taking the C_v values for lithium calculated from the measurements of Simon and Swain (19) by Kelly and MacDonald (9), values of V, the volume occupied by 1 gm. molecule, from the present work, and values of β, the compressibility, calculated from Bridgman's (6) measurements at 75° and 30° C., assuming (in the absence of other data) a linear temperature variation. The line plotted in Fig. 2 is calculated from these expansion coefficients, normalized to a value of 3.5019 kX at 295° K., and shows satisfactory agreement with the measured lattice parameters over the range 77° to 300° K. The γ value of 0.92 is considerably lower than 1.17 given by Mott and Jones (14). Further discussion is not possible until the exact temperature dependence of β has been established for the temperature range investigated.

Simon and Bergmann (18) obtained very good agreement of calculated and measured expansion coefficients using the Grüneisen relationship and C_v values corresponding to a $\theta_D = 510°$ C. (Simon and Swain's (19) specific heat measurements lead to an almost constant value of θ_D of $400° \pm 15°$ K. for lithium at temperatures from 100° to 300° K. (Kelly and MacDonald (9).) Kelly and MacDonald have pointed out that lithium is anomalous in that above 100° K. θ_R (resistance) is smaller than θ_D (specific heat). The inclusion of a Schottky transition leading to a higher intrinsic θ_D value, suggested by Simon and Bergmann as a result of their expansion coefficient measurements, would rather accentuate the anomaly $\theta_R < \theta_D$ since presumably a Schottky transition would not affect the electrical resistance.

In order to examine further the reported Martensitic transition (Barrett and Trautz (3)), b.c.c. Li $\rightarrow$ h.c.p. Li, two photographs were taken at tempera-

tures approaching that of liquid helium by running a stream of liquid helium from a syphon directly over the rotating specimen using the apparatus shown in Fig. 1. The helium flow was adjusted to maintain a thermocouple touching the specimen just below the X-ray beam axis at a constant temperature which was the lowest that could be obtained no matter how fast the helium flow was made. The temperature of the specimen was believed to be not greatly above 4° K.

The main fact to emerge from this experiment was that the b.c.c. form was still present to a large extent at these temperatures. The lattice parameter of the b.c.c. form at $\backsim 4°$ K. is $3.472_5 \pm .002$ kX (Fig. 2). Only limited information could be gained about the h.c.p. phase because of the probable coincidence of reflections (102), (104), (203, 120), (114, 122), etc., with those of the b.c.c. form, and (100), (101, 002), (200, 103) with those of Li_2O and possibly LiOH if either of these were present as impurities. However, its presence could certainly be inferred from the (110) and (201, 112) reflections of medium and weak intensity respectively at $\backsim 29.7°$ and $36.6° \theta$, which were free from the possibility of overlaps. Similar relative displacements of the interplanar spacings of the h.c.p. phase to those recorded by Barrett and Trautz (3) are found and these have been shown by Barrett (2) to be due to the presence of stacking faults.

It could not be definitely established whether there was any of the h.c.p. phase present in specimens photographed at 77.5° K.

ACKNOWLEDGMENT

The author's thanks are due to Mr. W. Stockdale for the spectrochemical analysis, Miss B. J. Anderson for able assistance with the practical work, and to Dr. D. K. C. MacDonald and Dr. J. S. Dugdale for discussions of problems of low temperature physics.

REFERENCES

1. Aruja, E. and Perlitz, H. Phil. Mag. 30: 55. 1940.
2. Barrett, C. S. Phase transformations in solids. John Wiley & Sons, Inc., New York. 1948. p. 351.
3. Barrett, C. S. and Trautz, O. R. Am. Inst. Mining Met. Engrs. Metals Technol. TP 2346. April, 1948.
4. Basinski, Z. S. and Christian, J. W. J. Inst. Metals, 80: 659. 1951–52.
5. Bijl, D. and Pullan, H. Phil. Mag. 45 (7): 290. 1954.
6. Bridgman, P. W. The physics of high pressure. G. Bell & Sons, Ltd., London. 1949. p. 160.
7. Ebert, H. Z. Physik, 47: 712. 1928.
8. Hume-Rothery, W. and Strawbridge, D. J. J. Sci. Instr. 24: 89. 1947.
9. Kelly, F. M. and MacDonald, D. K. C. Can. J. Phys. 31: 147. 1953.
10. Lipson, H. and Wilson, A. J. C. J. Sci. Instr. 18: 144. 1941.
11. Lonsdale, K. and Hume-Rothery, W. Phil. Mag. 36 (7): 799. 1945.
12. Lonsdale, K. and Smith, H. J. Sci. Instr. 18: 133. 1941.
13. MacDonald, D. K. C. and Pearson, W. B. Proc. Roy. Soc. (London), A, 221: 534. 1954.
14. Mott, N. F. and Jones, H. The theory of the properties of metals and alloys. Oxford University Press, London. 1936. p. 318.
15. Nelson, J. B. and Riley, D. P. Proc. Phys. Soc. (London), 57: 160. 1945.
16. Nix, F. C. and MacNair, D. Phys. Rev. 60: 597. 1941.
17. Post, B., Schwartz, R. S., and Fankuchen, I. Rev. Sci. Instr. 22: 218. 1951.
18. Simon, F. E. and Bergmann, R. Z. physik. Chem. B, 7: 268. 1930.
19. Simon, F. E. and Swain, R. C. Z. physik. Chem. B, 28: 189. 1935.

RADIATION FROM A SLOT ON A CYLINDRICALLY TIPPED WEDGE[1]

By James R. Wait and Sidney Kahana

ABSTRACT

A solution is outlined for the electromagnetic field of a distribution of magnetic current and charge in a volume bounded by an infinite wedge with a cylindrical tip both of infinite conductivity. The result is applied to calculate the fields of a thin half-wave transverse slot on the cylindrical surface. Radiation patterns in the equatorial plane are calculated for wedge angles of 90°, 180°, and 270° for various radii of the cylindrical surface. The results have application to the design of slotted cylinder antennas for directional coverage.

INTRODUCTION

Extensive use is now being made of the radiating properties of slots cut in the surface of a metal cylinder. Slotted cylinder antennas are particularly useful at very high and ultra-high frequencies to obtain broad coverage (5, 8, 6). For the particular case of an axial slot, Sinclair (9) has shown that the radiation pattern in the horizontal is essentially circular if the diameter of the cylinder is less than about a quarter of a wavelength. The pattern becomes more directive as the diameter of the cylinder is increased. A means thereby exists by which the horizontal pattern can be controlled to some extent. Sinclair also shows that a variety of patterns can be obtained by feeding power of different amounts to a pair of axial slots on the periphery of the cylinder.

An alternative method, suggested by Alford (1), to control the radiation pattern of slotted cylinders is to employ metal wings on the slots. The main effect of this "V" shaped reflector is to intercept the current which normally flows around the cylinder and to force it into the wings. The horizontal pattern is then rendered more directive with the radiation being confined mainly to the region subtended by the "V".

It is the purpose of this paper to derive expressions for the radiation of an arbitrary slot with a specified tangential voltage, on the cylindrical surface which is coaxial with an infinite corner reflector or wedge. This is an idealized theoretical model of the winged slots mentioned above. The solution of this problem may also be of interest in connection with slots radiating from airfoil and tail surfaces of aircraft. The final results are quite similar to the expressions derived by Papas (5) and Silver and Saunders (8) which are restricted to slots on isolated cylinders.

THE FORMAL SOLUTION

The general problem is to calculate the fields at P (see Fig. 1) due to a magnetic current element at P' with respect to a conducting wedge of angle ψ with a cylindrical tip of radius a. Choosing a cylindrical polar coordinate system, the surfaces of the wedge are defined by $\phi = 0$ and $\phi = \psi$, the tip

[1]*Manuscript received August 13, 1954.*
Contribution from Radio Physics Laboratory, Defence Research Board, Ottawa.

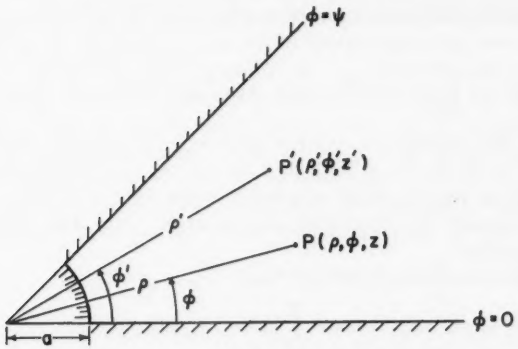

FIG. 1. Wedge with cylindrical tip.

by a cylindrical surface defined by $\rho = a$, $0 \leqslant \phi \leqslant \psi$, and the coordinates of P and P' are (ρ, ϕ, z) and (ρ', ϕ', z') respectively. The solution of the problem is most readily carried out by a Green's function method. Expressions for the field vectors are then obtained in terms of the currents and charges in the region and the fields on the surfaces of the region. In this particular problem it is more convenient to deal with magnetic currents and fictitious magnetic charges rather than their more conventional electric counterparts.

Following Stratton (10) it is readily shown that the electric and magnetic field vectors at P, $\mathbf{E}(r)$ and $\mathbf{H}(r)$, within a region V bounded by a surface S (with outward normal $\mathbf{n}$) are given by

$$[1] \quad \mathbf{H}(r) = \int_V \left[(-i\epsilon\omega)\mathbf{J}^*(r')G(r, r') + \frac{1}{\mu}\rho^*(r')\nabla' G(r, r') \right] dv'$$

$$- \int_S \{ i\omega\epsilon[\mathbf{n} \times \mathbf{E}(r')]G(r, r') + [\mathbf{n} \times \mathbf{H}(r')] \times \nabla' G(r, r') + [\mathbf{n} \cdot \mathbf{H}(r')]\nabla' G(r, r') \} da'$$

and

$$[2] \quad \mathbf{E}(r) = - \int_V [\mathbf{J}^*(r') \times \nabla' G(r, r')] dv'$$

$$+ \int_S \{ i\mu\omega[\mathbf{n} \times \mathbf{H}(r')]G(r, r') - [\mathbf{n} \times \mathbf{E}(r')] \times \nabla' G(r, r') - [\mathbf{n} \cdot \mathbf{E}(r')]\nabla' G(r, r') \} da'$$

where $\mathbf{J}^*(r')$ and $\rho^*(r')$ are the magnetic current density vector and magnetic charge at the point P'. The operator ∇' involves differentiation with respect to the primed coordinates. The Green's function $G(r, r')$ satisfies the inhomogeneous Helmholtz equation

$$[3] \quad (\nabla^2 + k^2) G(r, r') = -\delta(r - r')$$

where $\delta(r - r')$ is the three-dimensional Dirac function (3). It has been assumed in the above that the time factor is $\exp(i\omega t)$ and the medium contained in the volume V is homogeneous with electrical constants ϵ and μ.

To simplify the form of equations [1] and [2] it is convenient to impose

certain boundary conditions on $\partial G(r, r')/\partial n$ or $G(r, r')$ over the surface S. For example the axial component of the magnetic field can be written

$$[4] \qquad H_z(r) = \int_V \left[-i\epsilon\omega \, \mathbf{J}^*(r')G(r, r') + \frac{1}{\mu} \rho^*(r')\nabla' G(r, r') \right]_z dv'$$

subject to the conditions $\partial G(r, r')/\partial \rho' = 0$ at $\rho = a$, $0 \leqslant \phi \leqslant \psi$, and $\partial G(r, r')/\partial \phi' = 0$ at $\phi = 0$ and ψ, $a \leqslant \rho \leqslant \infty$. The integration over S is therefore seen to vanish, which is a result of the assumed perfect conductivity on the wedge and the vanishing contribution from the closing spherical surface at infinity.

With similar reasoning it follows that

$$[5] \qquad E_z(r) = -\int_V [\mathbf{J}^*(r') \times \nabla' G(r, r')]_z dv'$$

subject to $G(r, r') = 0$ at $\rho = a$, $0 \leqslant \phi \leqslant \psi$ and $\phi = 0$ and ψ, $a \leqslant \rho \leqslant \infty$.

The essential task at this stage is to find the forms of the Green's function which satisfy the above-mentioned boundary conditions. It can be seen that $G(r, r')$ can be written in the following general form

$$[6] \qquad G(r, r') = \frac{1}{2\pi} \int_{-\infty}^{+\infty} e^{-ih(z-z')} dh \times \sum_{m=0}^{\infty} \epsilon_m G_m(\rho, \rho', h) \frac{1}{2\psi} \left[\frac{\cos m\pi(\phi - \phi')}{\psi} \pm \frac{\cos m\pi(\phi + \phi')}{\psi} \right]$$

where the $+$ sign is employed for $\partial G(r, r')/\partial \phi' = 0$ at $\phi' = 0, \psi$ and the $-$ sign is employed for $G = 0$ at $\phi' = 0, \psi$ and $\epsilon_0 = 1$, $\epsilon_m = 2$ $(m \neq 0)$. The Fourier coefficient G_m is seen to satisfy the following inhomogeneous equation

$$[7] \qquad \left[\frac{\partial}{\partial \rho} \left(\rho \frac{\partial}{\partial \rho} \right) + (k^2 - h^2)\rho - \left(\frac{m\pi}{\psi} \right)^2 \frac{1}{\rho} \right] G_m(\rho, \rho', h) = -\delta(\rho - \rho')$$

which for points $\rho \neq \rho'$ is Bessel's equation of order $m\pi/\psi$. Solutions of equation [7] which are continuous at $\rho = \rho'$, give rise to outgoing waves at infinity, and satisfy the boundary condition that $\partial G/\partial \rho' = 0$ at $\rho' = a$ are

$$[8] \qquad G_m(\rho, \rho', h) = C_m H_\nu^{(2)}(u\rho) \left[J_\nu(u\rho') - \frac{H_\nu^{(2)}(u\rho')}{H_\nu^{(2)'}(ua)} J'_\nu(ua) \right] \quad \text{for } \rho > \rho'$$

or

$$[9] \qquad G_m(\rho, \rho', h) = C_m H_\nu^{(2)}(u\rho') \left[J_\nu(u\rho) - \frac{H_\nu^{(2)}(u\rho)}{H_\nu^{(2)'}(ua)} J'_\nu(ua) \right] \quad \text{for } \rho < \rho'$$

where $u = (k^2 - h^2)^{\frac{1}{2}}$, $\nu = m\pi/\psi$, J_ν is the Bessel function of the first type of order 2, and $H_\nu^{(2)}$ is the Hankel function of the second kind of order 2. The primes on the Bessel function indicate a differentiation with respect to the argument. The corresponding form of G_m to satisfy the boundary condition $G = 0$ at $\rho' = a$ is identical to equations [8] and [9] when the primes on the Bessel functions are removed. The factor can be found by integrating with respect to ρ on both sides of equation [7] over a small interval which includes ρ'. This process yields $C_m = -i\pi/2$. The formal solution of the problem is

then obtained when the required expressions for the Fourier coefficients are substituted into equation [6].

A particular application of this result is to calculate the fields of a distribution of magnetic current on the surface of the cylinder. By Schelkunoff's equivalence principle (7) such a distribution is equivalent to a specified tangential electric field on the surface of the cylinder. The process to obtain this special result is straightforward if it is remembered that an equation of continuity relates the magnetic charge and the magnetic current vector. It is also convenient to make use of the Wronksian relation (2)

$$[10] \qquad H_\nu^{(2)}(\alpha)\frac{\partial}{\partial\alpha}J_\nu(\alpha)-\frac{\partial}{\partial\alpha}H_\nu^{(2)}(\alpha)J_\nu(\alpha)=\frac{2i}{\pi\alpha}$$

when the transition is made from $\rho' \to a$ in the Green's function. Omitting further details of the derivation it follows from equations [4] and [5] that

$$[11] \qquad E_z(r)=\sum_{m=0}^{\infty}\epsilon_m\int_{-\infty}^{+\infty}a_m(h)H_\nu^{(2)}(u\rho)\,e^{-thz}\sin\nu\phi(k^2-h^2)\,dh$$

and

$$[12] \qquad H_z(r)=\sum_{m=0}^{\infty}\epsilon_m\int_{-\infty}^{+\infty}b_m(h)H_\nu^{(2)}(u\rho)\,e^{-thz}\cos\nu\phi(k^2-h^2)\,dh.$$

The coefficients a_m and b_m which are functions of h are related to the prescribed electric field components $E_z(a, \rho, z)$ and $E_\phi(a, \rho, z)$ on the portion of the surface of the cylinder defined by $z_1 \leqslant z \leqslant z_2$, $\phi_1(z) \leqslant \phi \leqslant \phi_2(z)$. The explicit forms of these coefficients are given by

$$[13] \qquad a_m(h)=\int_{z_1}^{z_2}dz'\int_{\phi_1(z')}^{\phi_2(z')}\frac{E_z(a,\,\phi',\,z')\,e^{thz'}\sin\nu\phi'\,d\phi'}{2\pi\,\psi\,H_\nu^{(2)}(ua)(k^2-h^2)}$$

and

$$[14] \qquad i\mu\omega b_m(h)=\int_{z_1}^{z_2}dz'\int_{\phi_1(z')}^{\phi_2(z')}\left[\frac{E_z(a,\,\phi',\,z')\,e^{thz'}\sin\nu\phi'(ih\nu)}{a(k^2-h^2)}+E_\phi(a,\,\phi',\,z')\,e^{thz'}\cos\nu\phi'\right]\frac{d\phi'}{2\pi\,\psi\,\partial H_\nu^{(2)}(ua)/\partial a}.$$

The remaining field components can be derived by the same process or they can be obtained directly from equations [11] and [12] if it is noted that the field can always be represented (11) as a basic set of TM (transverse magnetic) and TE (transverse electric) waves. They are given by

$$[15] \qquad E_\phi=\sum_{m=0}^{\infty}\epsilon_m\int_{-\infty}^{+\infty}\left[-\frac{ih}{\rho}a_m(h)\nu\,H_\nu(u\rho)+i\omega\mu b_m(h)\frac{\partial H_\nu^{(2)}(u\rho)}{\partial\rho}\right]e^{-thz}\cos\nu\phi\,dh,$$

$$[16] \qquad E_\rho=\sum_{m=0}^{\infty}\epsilon_m\int_{-\infty}^{+\infty}\left[-iha_m(h)\frac{\partial H(u\rho)}{\partial\rho}+\frac{i\mu\omega}{\rho}b_m(h)\nu H_\nu^{(2)}(u\rho)\right]e^{-thz}\sin\nu\phi\,dh,$$

$$[17] \qquad H_\phi=\sum_{m=0}^{\infty}\epsilon_m\int_{-\infty}^{+\infty}\left[-\frac{ik^2}{\mu\omega}a_m(h)\frac{\partial H_\nu^{(2)}(u\rho)}{\partial\rho}+\frac{ih\nu}{\rho}b_m(h)H_\nu^{(2)}(u\rho)\right]e^{-thz}\sin\nu\phi\,dh,$$

$$[18] \qquad H_\rho=\sum_{m=0}^{\infty}\epsilon_m\int_{-\infty}^{\infty}\left[\frac{ik^2}{\mu\omega\rho}a_m(h)\nu H_\nu^{(2)}(u\rho)-ihb_m(h)\frac{\partial H_\nu^{(2)}(u\rho)}{\partial\rho}\right]e^{-thz}\cos\nu\phi\,dh.$$

The integrations with respect to h can now be carried out under the usual far field approximation where terms of order $1/R^2$ and higher are neglected. The results of this saddle-point integration (12), expressed in terms of spherical polar coordinates (R, θ, ϕ), are

$$[19] \qquad E_\theta \simeq -2ik^2 \sin\theta \sum_{m=0}^{\infty} \epsilon_m a_m(k \sin\theta)\, e^{\frac{1}{2}i\nu\pi} \sin \nu\phi \frac{e^{-ikR}}{R},$$

$$[20] \qquad E_\phi \simeq 2i\mu\omega k \sin\theta \sum_{m=0}^{\infty} \epsilon_m b_m(k \sin\theta)\, e^{\frac{1}{2}i\nu\pi} \cos \nu\phi \frac{e^{-ikR}}{R},$$

$$H_\theta \simeq -\frac{k}{\mu\omega} E_\phi, \qquad H_\phi \simeq \frac{k}{\mu\omega} E_\theta$$

where $R = \sqrt{(\rho^2+z^2)}$ and $\tan\theta = \rho/z$.

Inserting the values of the coefficients, a_m and b_m, the radiation fields are given by

$$[21] \quad E_\theta = -\frac{i}{\pi\psi \sin\theta} \frac{e^{-ikR}}{R} \sum_{m=0}^{\infty} \frac{\epsilon_m e^{\frac{1}{2}i\nu\pi} \sin \nu\phi}{H_\nu^{(2)}(ka \sin\theta)} \int_{z_1}^{z_2} dz' \times \int_{\phi_1(z')}^{\phi_2(z')} E_z(a, \phi', z')\, e^{ikz\cos\theta z'} \sin \nu\phi'\, d\phi'$$

and

$$[22] \quad E_\phi = \frac{1}{\pi\psi} \frac{e^{-ikR}}{R} \sum_{m=0}^{\infty} \frac{\epsilon_m e^{\frac{1}{2}i\nu\pi} \cos \nu\phi}{H_\nu^{(2)'}(ka \sin\theta)} \times \left[\int_{z_1}^{z_2} dz' \int_{\phi_1(z')}^{\phi_2(z')} \left\{ E_\phi(a, \phi', z') \cos\nu\phi' + \frac{i\nu \cos\theta}{ka \sin^2\theta} E_z(a, \phi', z') \sin\nu z' \right\} e^{ikz\cos\theta z'} d\phi' \right].$$

It is apparent that the E_θ component of the radiation field depends only on the axial electric field $E_z(a, \phi, z)$ in the slot. It is also seen that this axial slot voltage also produces a transverse component E_ϕ of the radiation field. On the other hand the transverse electric field $E_\phi(a, \phi, z)$ in the slot produces only an E_ϕ component of the radiation field.

THIN $\lambda/2$ TRANSVERSE SLOT

The above general result can now be specialized to a thin slot of width w extending from $\phi = \phi_1$ to ϕ_2 at $z = z_0$ in a plane transverse to the axis of the cylinder (see Fig. 2). It can be assumed that if the slot is sufficiently thin the voltage distribution $V(\phi)$ varies sinusoidally along the slot, that is

$$[23] \quad V(\phi) = \int_{z_0-\frac{1}{2}w}^{z_0+\frac{1}{2}w} E_z(a, \phi, z)\, dz = wE_z(a, \phi, z_0) = V_0 \cos[ka(\phi'-\psi/2)]$$

for a slot centered at $\phi = \psi/2$, where V_0 is the voltage at the center of the slot. As a further consequence of the assumption of a very thin slot it can be seen that the contribution from the transverse voltage which is proportional to $E_\phi(a, \phi, z)$ is vanishingly small. The radiation fields of the thin half-wave transverse slot centered on the bisector of the wedge and located at $z = z_0$ on the cylindrical surface are then given by

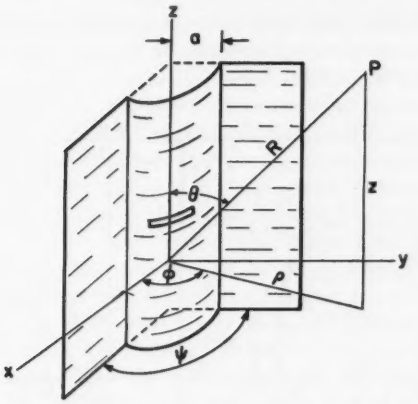

FIG. 2. Transverse slot of width w extending from ϕ_1 to ϕ_2 on surface of cylinder at $z = z_0$.

$$[24] \quad E_\theta = -\frac{ie^{-ikR}e^{ikz_0\cos\theta}}{\pi\psi\, R\sin\theta} V_0 ka \sum_{m=1,3,5,\ldots}^{\infty} \frac{4\sin\nu\phi\sin\frac{1}{2}m\pi\cos(\nu\pi/2ka)\, e^{\frac{1}{2}i\nu\pi}}{[(ka)^2-\nu^2]H_\nu^{(2)}(ka\sin\theta)},$$

$$[25] \quad E_\phi = \frac{ie^{-ikR}e^{ikz_0\cos\theta}V_0\cos\theta}{\pi\,\psi\, R\sin^2\theta} \sum_{m=1,3,5}^{\infty} \frac{4\nu\cos\nu\phi\sin\frac{1}{2}m\pi\cos(\nu\pi/2ka)\, e^{\frac{1}{2}i\nu\pi}}{[(ka)^2-\nu^2]H_\nu^{(2)'}(ka\sin\theta)},$$

where $\nu = m\pi/\psi$.

It is noted that in the equatorial plane (i.e. $\theta = 90°$) the E_ϕ component vanishes leaving only the E_θ component of the field. The radiation pattern proportional to $|E_\theta|^2$ in this plane is called the principle pattern of the trans-

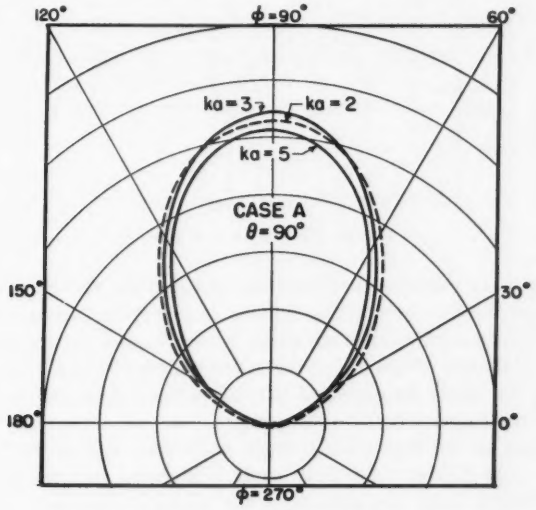

FIG. 3. Pattern for transverse slot on isolated cylinder.

verse slot. The following cases have been calculated: $ka = 2, 3$, and 5 and wedge angles ψ of $\pi/2$, π, and $3\pi/2$. These results along with those for an isolated cylinder are illustrated in Figs. 3 to 6.

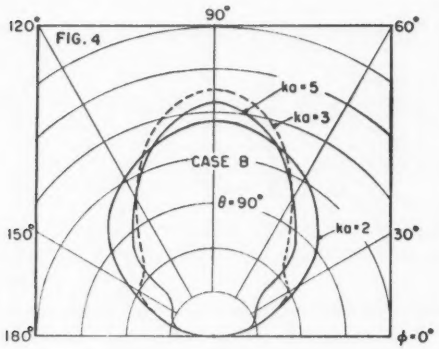

FIG. 4. Pattern for $\psi = 180°$.

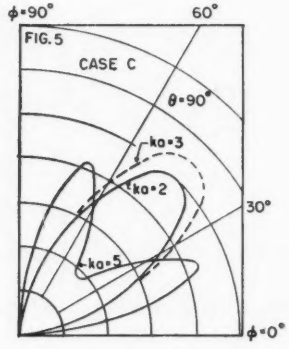

FIG. 5. Pattern for $\psi = 90°$.

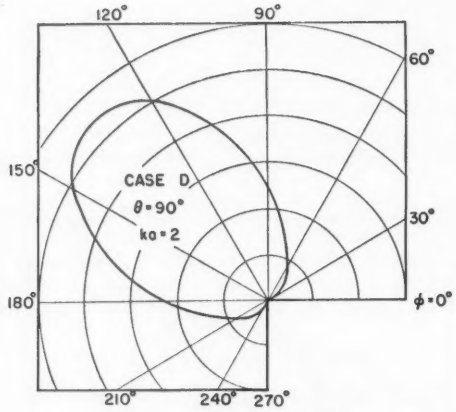

FIG. 6. Pattern for $\psi = 270°$.

The shape of the patterns is rather interesting. When the cylinder is isolated with no wedge, the field behind the cylinder is seen to be considerably reduced relative to the forward field. This effect is much more pronounced than for the case of axial slots where the patterns are almost circular in the equatorial plane (8, 9). As would be expected the diffraction effects become more pronounced for the larger circular cylinders.

The patterns for the slot on the cylinder with the wedge or the "V" reflector present are quite different. In these cases it is noted that the field is always zero in directions along the surface of the wedge, which is compatible with

the boundary condition that the tangential electric field is zero on these surfaces. An important feature of these patterns for the wedge is that for larger values of ka, multiple lobes can occur, which are usually undesirable.

The rigorous extension of the above theory to a wedge or reflector of finite extent would be very difficult indeed, if not impossible, by present-day techniques. It is believed, however, that the assumption of an infinite reflector does not limit the practical application of the results as much as at first sight. The effect of diffraction around the extremities of the reflector is somewhat similar to the case of a vertical electric antenna parallel to the apex of a corner reflector (13) where it has been observed experimentally (4) that the magnitude of the spurious field behind the reflector is within a few per cent of the central maximum if the reflector is made up of square sheets of dimensions greater than two wavelengths. In fact, consideration of knife edge diffraction would predict that the field behind the reflector in the equatorial plane would be of the order of $(kl)^{-3/2}$ times the central field, where l is the length of a side of the sheet.

REFERENCES

1. ALFORD, A. Proc. Natl. Electronics Conf. 2: 143. 1946.
2. ERDÉLYI, A., MAGNUS, W., OBERHETTINGER, F., and TRICOMI, F. G. Higher transcendental functions. Vol. 2. McGraw-Hill Book Company, Inc., New York. 1953. p. 80.
3. MORSE, P. M. and FESHBACH, H. Methods of theoretical physics. Vol. II. McGraw-Hill Book Company, Inc., New York. 1953.
4. MOULLIN, E. B. J. Inst. Elec. Engrs. (London), Pt. III, 92: 58. 1945.
5. PAPAS, C. H. J. Math. and Phys. 28: 227. 1950.
6. PISTOLKORS, A. A. J. Tech. Phys. (U.S.S.R.), 17: 377. 1947.
7. SCHELKUNOFF, S. A. Electromagnetic waves. D. Van Nostrand Company, Inc., New York. 1943. p. 158.
8. SILVER, S. and SAUNDERS, W. K. J. Appl. Phys. 21: 153 and 745. 1950.
9. SINCLAIR, G. Proc. I.R.E. 36: 1487. 1948.
10. STRATTON, J. A. Electromagnetic theory. McGraw-Hill Book Company, Inc., New York. 1941. ff. 464.
11. STRATTON, J. A. Electromagnetic theory. McGraw-Hill Book Company, Inc., New York. 1941. p. 354.
12. VAN DER WAERDEN, B. L. Appl. Sci. Research, B, 2: 43. 1951.
13. WAIT, J. R. Can. J. Phys. 32: 365. 1954.

NOTE

AN EXPERIMENTAL STUDY OF BAND INTENSITIES IN THE FIRST POSITIVE SYSTEM OF N_2

III. QUANTITATIVE TREATMENT OF EYE ESTIMATES

By R. W. Nicholls

INTRODUCTION

It is the purpose of this note to examine what quantitative information may be obtained on molecular constants and source conditions from eye estimates of band intensities. Naturally, for the complete interpretation of a molecular spectrum in terms of these quantities, accurate intensity measurements of the bands are a primary requisite. Such measurements are however seldom available, and yet quite often eye estimates of band intensities have been reported together with vibrational analyses of band systems (5).

In spite of the recognized deficiencies of subjective estimates of intensities, it seems necessary to examine whether any quantitative information may be obtained from these estimates when no other data on intensities are available. This situation often occurs in the preliminary interpretation of low dispersion spectra of weak sources.

As an example, some eye estimates of intensities of the first positive system of N_2 have been considered and have been shown to yield substantially the same results, in so far as the behavior of electronic transition moment with internuclear separation is concerned, as were obtained in parts I (7) and II (8). In these papers, accurately measured band intensities were used together with 'Franck–Condon Factors' in a manner suggested by Fraser (2) to find the dependence of electronic transition moment upon internuclear separation.

GENERAL CONCEPTS

The integrated intensity $I(v'v'')$ of a band may be written as

$$I_{v'v''} = H N_{v'} q_{v'v''} \bar{R}_e^2(\bar{r}_{v'v''}) / \lambda_{v'v''}^4, \qquad [1]$$

where H is a constant depending upon the optical system and units employed, $q_{v'v''} = |\int \psi_{v'} \psi_{v''} dr|^2$ is the 'Franck–Condon Factor' of the $v' \rightarrow v''$ transition,* and the other symbols have been previously defined in I and II.

If the photographic plate used is working on the roughly linear region of its characteristic, the photographic density D_λ produced at the band may be written as**

$$D_\lambda = \gamma_\lambda [\log I_{v'v''} - \log I_{0\lambda}] \qquad [2]$$

**This terminology for the overlap integral square has been suggested by Bates (1). The vibrational transition probability may then be written as* $p_{v'v''} = |\int \psi_{v'} R_e(r) \psi_{v''} dr|^2 = R_e^2(\bar{r}_{v'v''}) q_{v'v''}$.

***If the band is sufficiently wide that the band head is more simple to measure than the whole band,* D_λ *may be defined as the band head density, and then* $I_{v'v''}$ *will be replaced in equation [2] by* $I_{0\lambda}$, *the intensity included in the band head. For bands of one system,* $I_{0\lambda}/I_{v'v''}$ *may be expected to be roughly constant from band to band and dependent on rotational temperature (4).*

where γ_λ is the contrast factor of the emulsion response, and $I_{0\lambda}$ is the inertia of the emulsion at wavelength λ. Further, if the action of the eye in estimating blackening B_λ be compared to that of the photocell in a microdensitometer, application of the Weber–Fechner law of sensory responses to stimuli suggests that the rough relationship existing between estimated blackening and photographic density is

$$B_\lambda = \text{const} + CD_\lambda, \tag{3}$$

where C is a constant which determines the scale (usually 1 to 10) adopted in estimation of the blackening.

Thus from equations [1], [2], and [3]

$$B_\lambda = \text{const} + \delta_\lambda[\text{const} + \log N_{v'} + \log q_{v'v''} - 4 \log \lambda_{v'v''} + 2 \log R_e(\bar{r}_{v'v''}) - \log I_{0\lambda}], \tag{4}$$

where $\delta_\lambda = C\gamma_\lambda$ is a modified contrast factor. For the purposes of the following discussion it will be assumed that adequate data on $q_{v'v''}$ (3), $\lambda_{v'v''}$ (5), and $\bar{r}_{v'v''}$ (2) are available.

METHOD

Equation [4] indicates that the following simple procedure may reasonably be used to determine, albeit somewhat crudely, $R_e(r)$ of the transition and $N_{v'}$ of the source from eye estimates of band intensities.

Criteria of Quantitative Significance

The subjective nature of the eye estimate, the possible variation of plate response with wavelength, and also, particularly at small dispersions, the possible unsuspected presence of underlying band structure of other systems make very necessary the establishment of some criteria of quantitative significance to be applied to the B_λ data before use.

Equation [4] suggests that these criteria may be applied in connection with plots for v'' progressions (v' = const) of B_λ versus $\log q_{v'v''} - 4 \log \lambda_{v'v''}$. If plate response were roughly constant over the wavelength range of bands in a progression, each plot would be expected to be linear, of slope δ_λ, and relatively spaced in ordinate appropriate to the influence of the $\log N_{v'}$ term. Scatter of points about the straight line for one progression would be due to the influence of the $\log R_e(r)$ term. Slow variation in plate sensitivity will tend to disturb the rough equality of slope from line to line while really unreliable estimates of intensity and also the presence of unsuspected underlying band structure will cause marked deviation of individual points from the lines of their progessions. This is also a useful way of uncovering, from an intensity point of view, unsuspected underlying bands.

Data for aberrant points that lie far from their respective lines should of course be rejected as untrustworthy. In regions where plate response is relatively constant across the wavelength range of the system, an average slope δ can then be found from the slopes of the plotted lines.

Determination of the Electronic Transition Moment $R_e(r)$

For the remaining B_λ data, plots should be made of

$$B_\lambda/\delta - \log q_{v'v''} + 4 \log \lambda_{v'v''} \text{ versus } \bar{r}_{v'v''}$$

for each of the v'' progressions. From equation [6] it will be seen that this is equivalent to plotting

$$2 \log R_e(\bar{r}_{v'v''}) + \log N_{v'} + \text{const versus } \bar{r}_{v'v''}$$

for each progression over the range of r appropriate to it. The plots for each progression will vary in relative ordinate owing to the log $N_{v'}$ term, and in order to show how 2 log $R_e(\bar{r}_{v'v''})$ varies with r over the range of r encountered by the whole system, a consistent displacement in ordinate must be applied to each of the plots to allow for the effect of the log $N_{v'}$ term, and to make it possible for a smooth curve to be drawn through the points so displaced. In this way the behavior of log $R_e(r)$ with r may be found, and only in cases where the resulting plot is a line parallel to the r axis is one led to believe that the electronic transition moment is probably independent of internuclear separation.

Determination of Vibrational Population $N_{v'}$

In cases when examination of the degree of vibrational excitation in the source which is consistent with the eye estimates is necessary, the following method may be used. From the scaled plot of 2 log $R_e(r)$ versus r described above, a value of 2 log $R_e(\bar{r}_{v'v''})$ for each band may be read from the smooth curve. According to equation [4] plots of

$$B_\lambda/\delta \text{ versus } \log q_{v'v''} - 4 \log \lambda_{v''} + 2 \log R_e(\bar{r}_{v'v''})$$

should, for v'' progressions, be linear, of slope unity, and displaced in ordinate from the $v' = 0$ line by $\log(N_{v'}/N_0)$. Thus the vibrational population may be found from these displacements and plotted as $\log(N_{v'}/N_0)$ versus v'. Such plots will show, by their tendency to, or departure from linearity, whether or not the vibrational excitation is roughly of Boltzman form and whether certain vibrational levels have been favored in population or depopulation.

EXAMPLE

While the above treatment has been applied with success to a number of band systems whose eye estimates are available, perhaps the best test of its valid use is seen in the comparison between the dependence of $R_e(r)$ upon r for the first positive system of N_2 found from accurately measured intensities as described in I and II and that found from eye estimates of intensity.

The eye estimates have been taken from Pearse and Gaydon's well-known compilation of data on molecular spectra (5). The estimates there recorded for this system are from two sources: (*a*) Poetker's (6) band head intensities (λ greater than about 7000 Å) measured thermoelectrically, and (*b*) Pearse and Gaydon's estimates of blackening of Profs. A. Fowler and R. J. Strutt's plates (λ less than about 7000 Å). When the test of significance described above was applied, it showed that these two sets of numbers could not be considered on the same scale as equally representative. Accordingly, the following discussion is confined solely to the eye estimates.

For these data, application of the test of significance led to the rejection of

eye estimates of the (4, 0), (4, 1), (5, 0), (6, 1), (7, 2), (8, 3), (10, 7), (11, 8), (12, 6), (12, 7), (12, 8), (12, 9) bands as quantitatively unreliable. For the remaining 15 bands the plots of $2 \log R_e(\bar{r}_{v'v''}) + \log N_{v'} + \text{const}$ versus $\bar{r}_{v'v''}$ were made and the rescaling procedure was employed. It was found that a representative straight line consistent with

$$R_e(r) = \text{const} \exp(-2.7r) \quad [5]$$

could be drawn through the rescaled data. It will be recalled that the comparative result obtained in II was

$$R_e(r) = \text{const} \exp(-3.02\, r). \quad [6]$$

It may also be mentioned briefly that for the second positive system of N_2 and for the first negative system of N_2^+, analysis of recently recorded integrated intensities (9) has led to substantially the same $R_e(r)$ curves for these systems as were obtained from an analysis of the eye estimate data (5).

This, together with the substantial agreement between equations [5] and [6], indicates that the method described in this note for treating eye estimates of band intensities can be used in some cases to obtain roughly the same trends of $R_e(r)$ with r as may be obtained when more accurate intensities are available.

Details of the application of this procedure to other band systems and to the rough evaluation of vibrational distributions will be published shortly.

This work was performed in connection with Contract AF 19(122)–470 held with the Air Force Cambridge Research Centre.

REFERENCES

1. BATES, D. R. Monthly Notices Roy. Astron. Soc. 112: 614. 1952.
2. FRASER, P. A. Can. J. Phys. 32: 515. 1954.
3. JARMAIN, W. R. and NICHOLLS, R. W. Can. J. Phys. 32: 201. 1954.
4. NICHOLLS, R. W. J. Opt. Soc. Amer. 43: 882. 1953.
5. PEARSE, R. W. B. and GAYDON, A. G. The identification of molecular spectra. 2nd ed. Chapman and Hall, Ltd., London. 1950.
6. POETKER, A. H. Phys. Rev. 30: 812. 1927.
7. TURNER, R. G. and NICHOLLS, R. W. Can. J. Phys. 32: 468. 1954.
8. TURNER, R. G. and NICHOLLS, R. W. Can. J. Phys. 32: 475. 1954.
9. WALLACE, L. V. Private communication.

RECEIVED AUGUST 3, 1954.
DEPARTMENT OF PHYSICS,
UNIVERSITY COLLEGE,
UNIVERSITY OF WESTERN ONTARIO,
LONDON, ONTARIO.

CANADIAN JOURNAL OF PHYSICS

Notes to Contributors

Manuscripts

(i) ***General.*** Manuscripts should be typewritten, double spaced, on paper 8½×11 in. **The original and one copy are to be submitted.** Tables (each typed on a separate sheet) and captions for the figures should be placed at the end of the manuscript. Every sheet of the manuscript should be numbered.

Style, arrangement, spelling, and abbreviations should conform to the usage of this journal. Names of all simple compounds, rather than their formulas, should be used in the text. Greek letters or unusual signs should be written plainly or explained by marginal notes. Superscripts and subscripts must be legible and carefully placed.

Manuscripts should be carefully checked before they are submitted; authors will be charged for changes made in the proof that are considered excessive.

(ii) ***Abstract.*** An abstract of not more than about 200 words, indicating the scope of the work and the principal findings, is required, except in Notes.

(iii) ***References.*** References should be listed **alphabetically by authors' names,** numbered, and typed after the text. The form of the citations should be that used in this journal; in references to papers in periodicals, titles should not be given and only initial page numbers are required. All citations should be checked with the original articles and each one referred to in the text by the key number.

(iv) ***Tables.*** Tables should be numbered in roman numerals and each table referred to in the text. Titles should always be given but should be brief; column headings should be brief and descriptive matter in the tables confined to a minimum. Numerous small tables should be avoided.

Illustrations

(i) ***General.*** All figures (including each figure of the plates) should be numbered consecutively from 1 up, in arabic numerals, and each figure referred to in the text. The author's name, title of the paper, and figure number should be written in the lower left corner of the sheets on which the illustrations appear. Captions should not be written on the illustrations (see Manuscript (i)).

(ii) ***Line Drawings.*** Drawings should be carefully made with India ink on white drawing paper, blue tracing linen, or co-ordinate paper ruled in blue only; any co-ordinate lines that are to appear in the reproduction should be ruled in black ink. Paper ruled in green, yellow, or red should not be used unless it is desired to have all the co-ordinate lines show. All lines should be of sufficient thickness to reproduce well. Decimal points, periods, and stippled dots should be solid black circles large enough to be reduced if necessary. Letters and numerals should be neatly made, preferably with a stencil (**do NOT use typewriting**), and be of such size that the smallest lettering will be not less than 1 mm. high when reproduced in a cut 3 in. wide.

Many drawings are made too large; originals should not be more than 2 or 3 times the size of the desired reproduction. In large drawings or groups of drawings the ratio of height to width should conform to that of a journal page but the height should be adjusted to make allowance for the caption.

The original drawings and one set of clear copies (e.g. small photographs) are to be submitted.

(iii) ***Photographs.*** Prints should be made on glossy paper, with strong contrasts. They should be trimmed so that essential features only are shown and mounted carefully, with rubber cement, on white cardboard.

As many photographs as possible should be mounted together (with a **very** small space between each photo) to reduce the number of cuts required. Full use of the space available should be made and the ratio of height to width should correspond to that of a journal page; however, allowance must be made for the captions. Photographs or groups of photographs should not be more than 2 or 3 times the size of the desired reproduction.

Photographs are to be submitted in duplicate; if they are to be reproduced in groups one set should be mounted, the duplicate set unmounted.

Reprints

A total of 50 reprints of each paper, without covers, are supplied free. Additional reprints, with or without covers, may be purchased.

Charges for reprints are based on the number of printed pages, which may be calculated approximately by multiplying by 0.6 the number of manuscript pages (double-spaced typewritten sheets, 8½ × 11 in.) and making allowance for illustrations (not inserts). The cost per page is given on the reprint requisition which accompanies the galley.

Any reprints required in addition to those requested on the author's reprint requisition form must be ordered officially as soon as the paper has been accepted for publication.

Contents

Page

The Potassium-Argon Method of Geological Age Determination—*H. A. Shillibeer and R. D. Russell* - - - - - - - - - 681

H-Plane Bifurcation of Rectangular Waveguides—*R. A. Hurd and H. Gruenberg* - - - - - - - - - - - - - - - 694

A Method of Concentrating He^3-He^4 Mixtures—*K. R. Atkins and D. R. Lovejoy* - - - - - - - - - - - - - - 702

Thermal Expansion of Lithium, 77° to 300°K.—*W. B. Pearson* - - 708

Radiation from a Slot on a Cylindrically Tipped Wedge—*James R. Wait and Sidney Kahana* - - - - - - - - - - - - 714

An Experimental Study of Band Intensities in the First Positive System of N_2. III. Quantitative Treatment of Eye Estimates—*R. W. Nicholls* - - - - - - - - - - - - - - 722

Printed in Canada *by* University of Toronto Press